CALIFORNIA STATE UNIVERSITY, NORTHRIDGE

TARGETED THERAPY OF LEUKEMIA STEM CELLS (LSCS) IN *PTEN*-DEFICIENT T-CELL ACUTE LYMPHOBLASTIC LEUKEMIA (T-ALL)

A thesis submitted in partial fulfillment of the requirements
For the degree of Master of Science in Biology

By

Anjelica Mia Cardenas

May 2014

ACKNOWLEDGEMENTS

I would like to thank Dr. H. Wu for generously hosting me in her cancer research laboratory at UCLA for the 2012 - 2013 CSUN - UCLA CIRM Bridges to Stem Cell Research Program. I would also like to thank my mentor, Dr. S. Schubbert, for her time and effort during my year of research and afterwards in the writing of this thesis. I am grateful for her patience and assistance with this thesis project and in the writing process. Thank you to C. Garcia, H. Chen, L. Ma, and J. Shi for technical assistance with experiments and assays. I would also like to thank my family and friends who were understanding and supportive throughout the entire process, all my colleagues for helpful discussion and comments, and I would especially like to thank my Thesis advisor, committee chair, and CIRM Bridges Director Dr. C. Malone for her guidance and assistance with both the program and this thesis. Thank you to Dr. M. Summers and Dr. L. Banner for being members of my Thesis Committee.

Dr. G. Cheng, Dr. A. Ferrando, Dr. C. Radu, and Dr. X. Chen generously provided human T-ALL cell lines: Jurkat, CCRF-CEM, MOLT3, MOLT4, and MOLT16. Dr. M. Dail generously provided murine cell lines: *Kras*WT 12-0, *Kras*WT 8608, *Kras*^{G12D} 9r, and TIMI.4 (41). In addition, Dr. J. Bradner kindly donated JQ1 and Dr. J. Yuan kindly donated A70 (40). This project was supported in funding by CSUN - UCLA Bridges to Stem Cell Research Program, TB1 - 01183. Dr. S. Schubbert was supported by the Leukemia and Lymphoma Society fellow award, National Cancer Institute of the NIH, T32 - CA009120 - 36, and the William Lawrence & Blanche Hughes Foundation.

TABLE OF CONTENTS

LIST OF TABLES AND FIGURES

ABSTRACT

TARGETED THERAPY OF LEUKEMIA STEM CELLS (LSCS) IN *PTEN*-DEFICIENT T-CELL ACUTE LYMPHOBLASTIC LEUKEMIA (T-ALL)

By

Anjelica Mia Cardenas

Master of Science in Biology

T-cell acute lymphoblastic leukemia (T-ALL) is a hematopoietic malignancy characterized by an overproduction of immature T-cell lymphocytes (blasts) and infiltration into bone marrow and peripheral blood. Deletion and mutation of the tumor suppressor gene, *Phosphatase and Tensin Homolog (PTEN),* a negative regulator of the PI3K/AKT/mTOR pathway, has been reported in a large percentage of T-ALL patients and is associated with relapse and poor prognosis. In this study, we utilized our previously generated genetic *VEC-Cre*$^{+}$*Pten* $^{loxP/loxP}$(*Pten* null) T-ALL murine model and recently derived *Pten* null T-ALL cell culture to evaluate the effects of potential combination therapies. *Pten* null T-ALL develops in this model after the activation of β-catenin and a chromosomal translocation of the *c-Myc* oncogene and the *T-cell antigen receptor (TCR) α/δ cluster* t(14;15) with subsequent Myc overexpression. Previous studies have shown treatment with the mTOR inhibitor, rapamycin, prolongs survival of *Pten* null T-ALL mice. However, rapamycin was insufficient to eradicate leukemia stem cells (LSCs), the defined leukemia-propagating subpopulation in this model, and cure T-ALL. Therefore, we hypothesize that a more effective approach to eliminate blasts, LSCs, and ultimately the disease in our *Pten* null T-ALL murine model and derived *Pten* null T-

ALL cell cultures would be to utilize combination therapy to simultaneously co-target essential alterations and key signaling pathways.

Since rapamycin alone has little effect on *Pten* null LSCs, we intend to eradicate the blasts and LSCs, by selectively targeting critical molecular and genetic abnormalities that have previously been defined as requirements for LSC formation and T-ALL development with dual drug treatment. Recently, small molecule inhibitorsVX-680, JQ1, and Purvalanol A have been shown to either directly regulate *Myc* expression or indirectly target cells with *Myc* overexpression. In addition, A70, a synthetic autophagy inhibitor, has been shown to prevent autophagy and may potentially sensitize *Pten* null T-ALL LSCs cells to rapamycin treatment. In this study, we co-targeted mTOR, the downstream target of the PI3K/AKT/mTOR signaling pathway and *Myc* overexpression utilizing rapamycin in combination with the selected small molecule inhibitors using both *in vivo* and *in vitro* models. We assessed the therapeutic efficacy of selected inhibitors and characterized the molecular mechanisms underlying their effects directed against both the PI3K/AKT/mTOR pathway and deregulated *Myc* expression. These deregulated pathways, critical for T-ALL development, are common alterations seen in human T-ALL.

CHAPTER 1: INTRODUCTION

Prologue

Acute lymphoblastic lymphomas and leukemias (ALLs) are a variety of white blood cell cancers defined by their rapid and aggressive onset of the disease in contrast to the slower development of chronic lymphoblastic lymphomas and leukemias (1). These neoplasms are commonly heterogeneous and occur in B- and T-lymphocyte progenitors following transformation from acquisitions of an assortment of genetic mutations (1). T-cell acute lymphoblastic leukemia (T-ALL) is a hematopoietic malignancy of T-lymphoid progenitor cells and occurs both in children and adults (2, 3). It is characterized by an overproduction of immature T-lymphocytes (also known as lymphoblasts or blasts) and their infiltration into bone marrow and peripheral blood. Frequently, T-ALL is associated with deregulated oncogene expression and chromosomal translocations (3). Common translocations that occur involve juxtaposition of promoter and enhancer regions of *T-cell receptor (TCR)* genes with transcription factors such as *HOX11*, *TAL1*, and *MYC* (4). These genetic alterations enhance or maintain the ability of these cells to self-renew, increase proliferation, and prevent differentiation (2, 3). While treatment regimens have improved in recent years, current treatments consist of multi-agent chemotherapy with substantial side effects. Approximately 25% of children and 50-70% of adult individuals with T-ALL develop treatment-resistant disease and those who relapse have poor prognosis (2-3, 5-6).

Malignant tumors commonly exhibit a heterogeneous composition, both morphologically and functionally (8-14). Cancer stem cells (CSCs) have been proposed as a subset of the tumor population responsible for tumor formation and maintenance

with traits similar to normal stem cells (8-14, 16). These CSCs are characterized by their ability to self-renew, generate or differentiate into other cell types within the tumor, and recapitulate the tumor of origin when transplanted (8-12). Genetic lesions within the CSCs are hypothesized to contribute to the mechanism by which these cells acquire stem-cell-like characteristics. The stem-cell properties are proposed to be responsible for tumor maintenance, promotion of metastasis, and may be responsible for therapeutic resistance (6, 10). However, these cells are not necessarily the "cell of origin" in the cancer. The cell of origin is considered to be the cell that first acquired a mutation followed by subsequent mutations which transform a normal cell to a malignant one (8-9, 11-12, 14, 16).

It has been shown in other types of leukemia, such as acute myeloid leukemia (AML), there is a population of leukemia-initiating cells termed leukemia stem cells (LSCs) that have the capacity to self-renew and differentiate into progenitor cells as well as initiate disease when transplanted into immuno-compromised mice (8-9, 11-12, 14-15). These LSCs have also been shown to be distinct from normal hematopoietic stem cells (HSCs) in *Pten*-deficient leukemias where *Pten* deletion resulted in HSC depletion but LSC generation (15). Following *Pten* deletion, LSCs develop in our *Pten*-deficient T-ALL murine model after β-catenin activation and a chromosomal translocation of the *c-Myc* oncogene and the *T-cell antigen receptor (TCR) α/δ cluster* t(14;15) with consequent Myc overexpression. LSCs were identified within our *Pten*-deficient T-ALL mouse model and characterized by well-defined surface markers and their ability to recapitulate the disease in immuno-deficient mice as the subpopulation that self-renews and initiates disease when transplanted.

Deletion and mutation of the tumor suppressor gene*, Phosphatase and Tensin Homolog (PTEN),* has been reported in many cancer types including a substantial percentage of patients with T-ALL (5-7, 15-18). PTEN negatively regulates the phosphatidylinositol-3-OH Kinase/AKT/mammalian target of rapamycin (PI3K/AKT/mTOR) transduction pathway and assists in the maintenance of genomic stability (6, 19). The PI3K/AKT/mTOR signal pathway promotes cellular processes that include cell growth, proliferation, and survival (6). PTEN, a lipid and protein phosphatase, dephosphorylates phosphatidylinositol 4, 5 phosphate 3 (PIP3) generating PIP2 (6, 19). PIP3 is a downstream target of PI3K that activates a cascade of signaling molecules of the PI3K pathway inhibiting apoptosis and positively regulating cell proliferation (9). *NOTCH Homolog 1 (NOTCH1)* mutations are common in human T-ALL and have been shown to regulate the expression of *PTEN* and its effects on the PI3K pathway (6, 17-18, 20). In a large portion of *NOTCH1* activated primary T-ALL samples, aberrant *PTEN* and PI3K/AKT/mTOR pathway genes were identified as secondary events in disease progression and associated with resistance to activated NOTCH1 inhibition (17). However, *Pten*-deficiency can occur independently of *NOTCH1* mutation in the pathogenesis of T-ALL (6, 20). It is important to understand the development of *PTEN*-deficient T-ALL, disease maintenance, and resistance to treatment in relapsed populations in order to develop and put forth improved therapy regimens.

Our lab has previously developed a genetic *Pten* null T-ALL murine model (6-7). In previous studies, it was shown the mTOR inhibitor, rapamycin, suppressed T-ALL development in pre-leukemic *Pten* null mice (6-7). However, rapamycin did not eradicate the established LSC population nor abolish T-ALL in *Pten* null mice with acute disease

(7). In this study, we utilize the *Pten* null T-ALL murine model and the recently derived *Pten* null T-ALL cell line to investigate therapeutic strategies that co-target key pathways specific to *Pten*-deficient LSCs. Utilization of combination therapies to target and exploit genetic lesions unique to *Pten* null LSCs may offer improved therapy to treat human *PTEN*-deficient T-ALL without harm to normal cells. We utilized small, synthetic inhibitors to selectively target required alterations for *Pten* null T-ALL development. We evaluated the therapeutic efficacy of direct and indirect *Myc* small molecule inhibitors, which include VX-680, JQ1, and Purvalanol A. Furthermore, we evaluated the efficacy of an autophagy inhibitor, A70 and the mTOR inhibitor, rapamycin, to investigate small molecule inhibitor effects on mechanisms of cell growth and survival in *Pten* null T-ALL.

Previous Work

Our lab developed a *VE-Cadeherin-Cre*$^{+}$;*Pten* $^{loxP/loxP}$;*Rosa*^{floxedSTOP}*; LacZ*$^{+}$ (*Pten* null) T-ALL genetic murine model (Fig. 1), in which the disease is conditionally initiated by the loss of *Pten* in HSCs. The mice briefly develop myeloproliferative disorder (MPD) followed by *Pten* null T-ALL with 100% penetrance by 2 - 3 months (6). Within the T-ALL hematopoietic population, LSCs (c-Kit^{mid} CD3^{+}) and blasts (c-Kit^{-}CD3^{+}) subpopulations were functionally defined when sorted and transplanted into severe combined immunodeficiency disease (SCID) mice. Mice transplanted with cKit^{mid}CD3^{+} cells efficiently recapitulated the disease in contrast c-Kit^{-}CD3^{+} cell populations (6). Therefore, the cKit^{mid}CD3^{+} cell population is enriched with disease-initiating and self-renewable LSCs in our *Pten* null T-ALL model

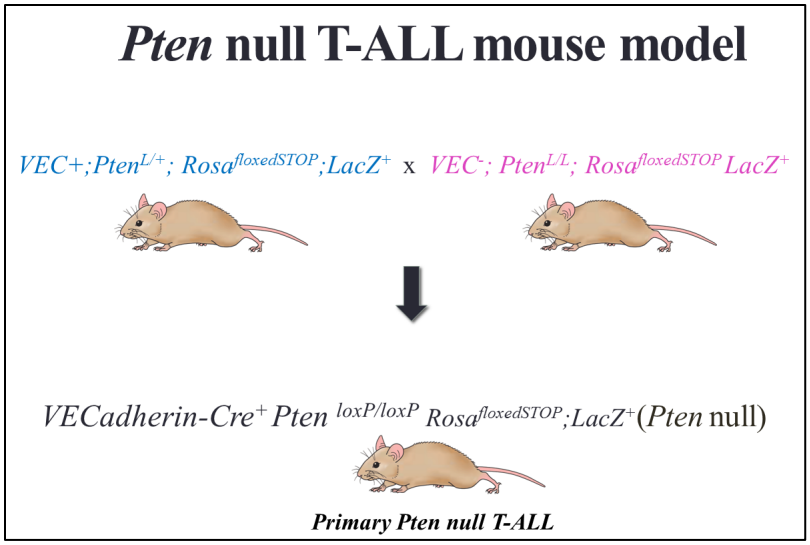

Figure 1: Schematic representation of the breeding used to generate our *Pten* null T-ALL mouse model. A male *VEC-Cre*$^{+}$*;Pten* $^{L/+}$ *;Rosa*^{floxedSTOP}*; LacZ*$^{+}$ is crossed with a *VEC-Cre*$^{-}$*;Pten*$^{L/L}$ *;Rosa*^{floxedSTOP}*; LacZ*$^{+}$ female in order to produce progeny including *VEC-Cre*$^{+}$*;Pten* $^{L/L}$ *;Rosa*^{floxedSTOP}*; LacZ*$^{+}$ primary *Pten* null T-ALL mice (must be *Pten*$^{L/L}$ for T-ALL).

Development of T-ALL in this model was found to occur after the acquisition of two spontaneous molecular changes following *Pten* deletion in HSCs. Leukemogenesis required both increased activation (increased levels of the unphosphorylated form) of β-catenin and a chromosomal translocation of the *c-Myc* oncogene and the *T-cell antigen receptor (TCR) α/δ* cluster t(14;15) (Fig. 2) (6). The increase of activated β-catenin may contribute to LSC's ability to self-renew (20) while the *TCRα/δ-c-Myc* translocation may promote aberrant T-lineage-specific overexpression of *c-Myc,* which may promote cell proliferation and entry into the cell cycle in our *Pten* null T-ALL model. Although *NOTCH1* mutations are common in human T-ALL, *Notch1* mutations were not identified in this model suggesting that loss of *PTEN* function and overexpression of *Myc* through the *TCRα/δ-c-Myc* translocation are sufficient to cause a distinct subset of T-ALL (20).

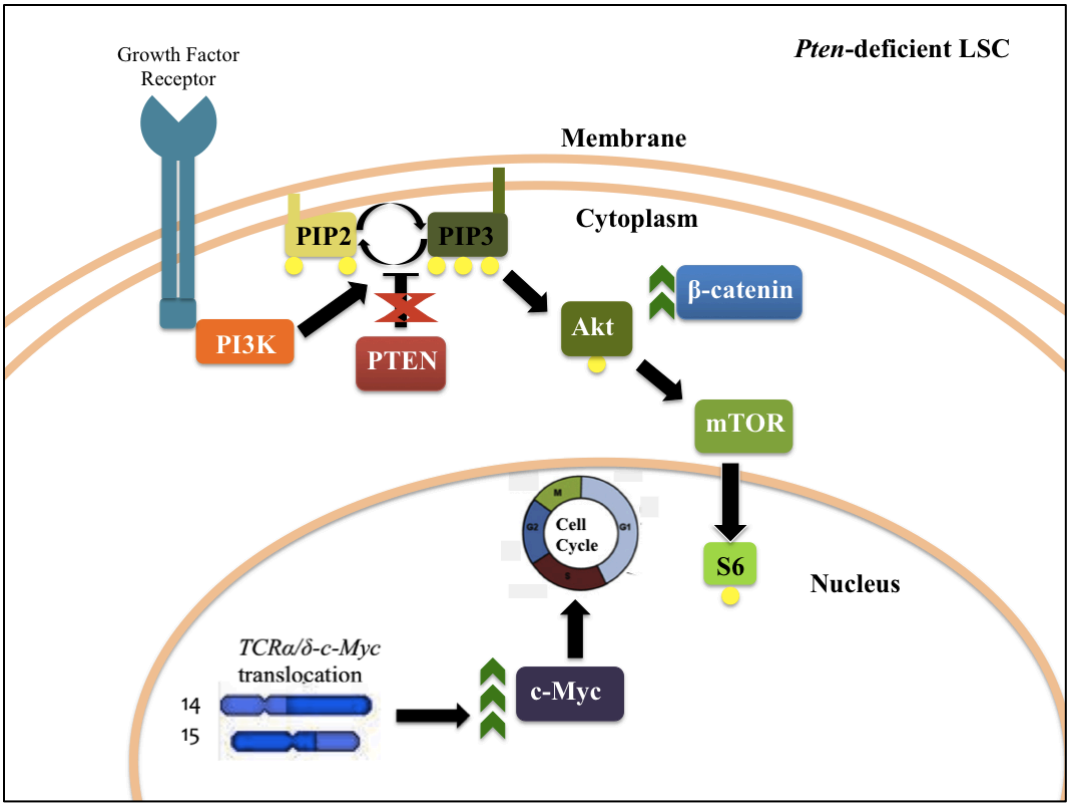

Figure 2: Schematic representation of deregulated pathways in our *Pten* null T-ALL model. Development of the disease begins with loss of *Pten* function and regulation of the PI3K/AKT/mTOR signaling pathway followed by subsequent β-catenin activation and a chromosomal translocation of the *T-cell antigen receptor (TCR) α/δ cluster* and the *c-myc* oncogene t(14;15).

In another study, our lab determined that loss of *Pten* with increased activation of β-catenin alone did not transform HSCs into disease-initiating LSCs (7). *Pten* null $CD4^{+}CD8^{+}$ double-positive (DP) thymocytes were identified as the population and stage in thymocyte development that is susceptible to the *TCRα/δ-c-Myc* translocation required for LSC transformation. Treatment with the mTOR inhibitor, rapamycin was utilized to block T-cell transformation at the double negative (DN) to DP stage of development in an attempt to prevent T-ALL in pre-leukemic *Pten* null mice (7). T-ALL mice treated with rapamycin were found to have a reduced blast population and prolonged lifespan (7). Rapamycin was able to prevent the formation of self-renewable LSCs and T-ALL

development in pre-leukemic mice, however, rapamycin did not eliminate existing LSCs in *Pten* null T-ALL mice who eventually relapsed and succumbed to the disease.

Hypothesis

Targeting one pathway by rapamycin treatment does not eradicate existing LSCs in *Pten* null T-ALL mice; therefore, we investigated the role of other essential pathways to potentially provide improved therapy. We hypothesized that a more effective approach to eliminate blasts, LSCs, and ultimately the disease in our *Pten* null T-ALL murine model and derived *Pten* null T-ALL cell line would be to utilize combination therapy to simultaneously co-target essential alterations and key signaling pathways (13). We sought to eradicate the blasts and the leukemia-propagating population, LSCs, by selectively targeting critical molecular and genetic abnormalities that have previously been defined as requirements for LSC formation and T-ALL development with dual drug treatment. We hypothesized this treatment would result in a synthetic lethal effect specific to our *Pten* null T-ALL cells and spare all other cells that do not have up-regulated Myc expression and deregulated PI3K/AKT/mTOR pathways. We propose the mTOR inhibitor, rapamycin, in combination with small molecules known to directly or indirectly target Myc expression may be a more effective therapeutic treatment approach for our *Pten* null T-ALL model and may offer improved therapies to treat human T-ALL (Fig. 3).

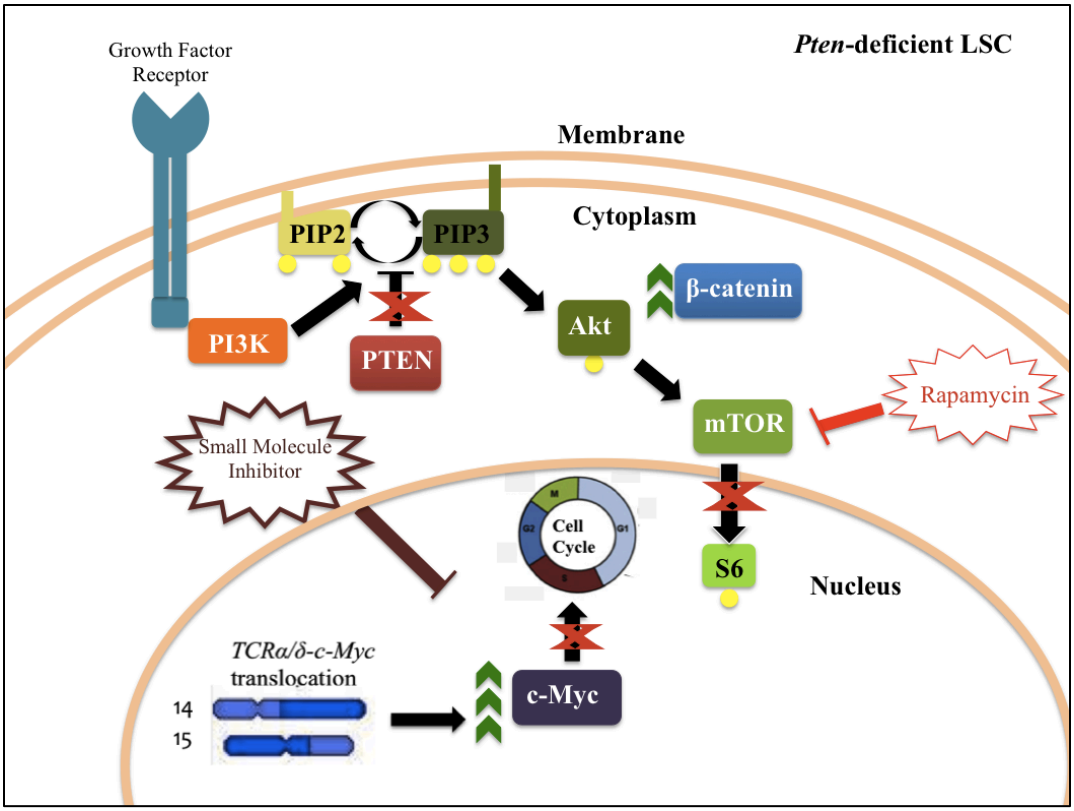

Figure 3: Schematic representation of our proposed targeted combination therapy. Co-targeting the PI3K/AKT/mTOR pathway with rapamycin and c-Myc over-expression using a small molecule inhibitor to eliminate blasts, LSCs, and ultimately *Pten* null T-ALL in our model.

Selected Small Molecule Inhibitors

The mTOR kinase is a downstream target of AKT and the intracellular target of the inhibitor, rapamycin. mTOR is a serine/threonine-protein kinase that makes up a portion of two independent complexes, mTORC1 and mTORC2 and directly regulates mRNA translation, lipid biosynthesis, autophagy, and mitochondrial biogenesis (21-23). mTORC1 phosphorylates S6 kinase and negatively regulates PI3K (23-24). mTORC2 phosphorylates AKT at Ser 473 (23). Rapamycin indirectly inhibits mTORC2 signaling; however, inhibition of mTORC1 prevents the negative feedback loop resulting in increased AKT phosphorylation and subsequent increased mTOR activation (22-23). Our previous studies utilized the agent rapamycin to uncover mTOR's role as a mediator in

the regulation of β-selection in *Pten;Rag1* null mice. Rapamycin was shown to alter nutrient sensing during β-selection and caused an arrest in the blast population at the DN3 stage (7). Rapamycin was used to prevent T-cell differentiation and leukemia formation in our pre-leukemic *Pten*-deficient T-ALL model. However, our *Pten* null T-ALL LSCs are not responsive to single agent rapamycin treatment (7). Targeting one pathway by rapamycin is not sufficient to eradicate *Pten* null T-ALL LSCs, therefore, it is important to co-target multiple pathways with inhibitors and investigate the effects of such combination treatment.

We selected c-Myc as a secondary target of our proposed combination therapy because *Myc* overexpression was previously determined to be required for LSC formation and leukemia development in our *Pten* null T-ALL model. *MYC* is a well-conserved proto-oncogene among a range of species (25) and evidence suggests when the protein is highly expressed, there is a correlation of an initiation of tumorgenesis in a variety of human cancers (26). The c-Myc protein is a transcription factor, a DNA binding protein that regulates gene expression (27), and has been shown localize in the nuclear region following transcription. Studies have found c-Myc target genes have roles in metabolism, apoptosis, and promotion of cell proliferation and cell cycle induction (28). Myc has been known to be difficult to inhibit directly, however, VX-680, JQ1, and Purvalanol A have been selected for our studies based on their ability to indirectly target cells with *Myc* overexpression or directly regulate *Myc* expression in other models. As an alternative dual drug treatment we have also selected the anti-autophagy agent, A70 to sensitize and target T-ALL cells in combination with rapamycin (Table 1). We utilize our genetic *Pten* null T-ALL mouse model and *Pten* null T-ALL *in vitro* cell line model to assess the

efficacy and molecular mechanism of these inhibitors alone and in combination with rapamycin to eliminate LSCs and cure T-ALL.

Small Molecule Inhibitors	Description
Rapamycin	• mTOR pathway inhibitor. • Prevents LSC formation and leukemia development in *Pten* null T-ALL pre-leukemic mice. • Cannot eliminate established *Pten* null LSCs. *Cao et al, 2006 Cancer Research; Guo et al, 2011 PNAS*
VX-680	• Aurora kinase inhibitor. • Blocks cytokinesis and mitosis. • Reported to be synthetic lethal in Myc over-expressing cells. *Harrington et al, 2004 Nature Medicine; Yang et al 2010 PNAS; den Hollander 2010 Blood*
JQ1	• Selective BET family of bromodomains inhibitor. • Reported to down-regulate *MYC* and *IL-7Rα* expression and decrease expression of *MYC* target genes. *Fillipakopoulos et al, 2010 Nature; Mertz et al, 2011 PNAS; Zuber et al, 2011 Nature; Dawson et al, 2011 Nature; Delmore et al, 2011 Cell Press; Ott et al, 2012 Blood*
Purvalanol A	• A cyclin-dependent kinase (CDK1) inhibitor. • Shown to down-regulate survivin expression and induce MYC-dependent apoptosis. *Goga, A., et al. 2007 Nature Medicine*
A70	• An anti-autophagy agent. • Shown to sensitize cancer lines to autophagy inhibition. *Liu, J. et al. 2011 Cell*

Table 1: Selected small molecule inhibitors.

VX-680 is a synthetic Aurora kinase inhibitor designed to be potent, selective, and reversible by targeting the ATP-binding site of the Aurora kinases (29-30). Aurora kinases are a family of conserved serine/threonine kinases that play an essential role in mitosis during cell cycle progression and are required for cytokinesis (29-32). Our lab has recently discovered that a large portion of *Pten* null T-ALL LSCs are in cycle (data not shown). Interestingly, VX-680 has been shown to interrupt cell cycle progression and block proliferation, cause polyploidy, and induce apoptosis and autophagy in cycling cells associated with malignancy and *Myc* overexpression both *in vitro* and *in vivo* (29). We have selected VX-680 to exploit *Myc* overexpression of our *Pten* null T-ALL since

Aurora A and Aurora B have been shown to be up-regulated by *Myc* expression in *Myc*-driven B-cell lymphoma and have been shown to be sensitive to Aurora kinase inhibition (31). Furthermore, VX-680 has been shown to have a synthetic lethal interaction with *Myc* overexpressing cells in various leukemias (30). In addition, non-cycling cells and otherwise normal cells remain unaffected since Aurora kinases are highly expressed only during G_2 and mitosis phases of cell cycle (29, 31). Together, these characteristics allow for VX-680 to be an ideal synthetic inhibitor for our proposed combination therapy.

The small molecule inhibitor, JQ1 has a high affinity for the bromodomain-containing 4 protein (Brd4), a member of the BET bromodomain-containing protein family that binds to acetylated histones and influences transcription by recruiting transcriptional activators (33-36, 38, 40). JQ1 does not bind bromodomains of proteins outside of this BET family and suppresses Brd4 activity by competitively binding to the acetyl-lysine binding domain of Brd4, which dissociates the protein from chromatin (33-37, 40). JQ1 has been selected since it has been shown to down-regulate *Myc* expression at various levels in a broad spectrum of leukemia cell lines, is potent and reversible as a single-agent, and is tolerated *in vivo* (33-40). Our *Pten* null T-ALL cell lines require Interleukin-7 (IL-7) supplemented media. JQ1 has been shown to down-regulate the cytokine IL-7 receptor (IL-7R) in B-cell acute lymphoblastic leukemia (37). The mechanism by which MYC and IL-7R expression is down-regulated correlates with depletion of BRD4 at the *MYC* and *IL-7R* promoter regions of chromatin in JQ1 treated cells (37) suggesting JQ1 as a possible pharmacological route to suppress *Myc* in our *Pten* null cells as well as utilizing another potential mechanism of LSC eradication by preventing IL-7R activity.

Purvalanol A is a cyclin-dependent kinase 1 (CDK1) inhibitor found to have synthetic lethal effects in *Myc* overexpressing cells (41). CDK1 is a protein kinase that regulates cell cycle progression in cells. CDK1-complex activity has been shown to increase in cells with *Myc* overexpression (32). The downstream target of CDK1, the BIRC5 protein (survivin), is an inhibitor for apoptosis and essential for survival in cells with *Myc* overexpression (41). Purvalanol A has been shown to induce apoptosis in cells that overexpress *Myc* through this CDK1 inhibition with subsequent survivin down-regulation (41). Purvalanol A has been selected for our studies because of its potential to sensitize cells to apoptosis induction by survivin depletion and the synthetic lethal interaction that is attributed to survivin. Since Purvalanol A inhibits the cell cycle, cycling cells will be affected while most normal, differentiated cells are not actively dividing but are in G_0/G_1, which should enable them to withstand the drug.

A70 is a synthetic derivative of specific and potent autophagy inhibitor-1 (spautin-1) from the lab of J. Yuan (42). This anti-autophagy inhibitor has been shown to inhibit autophagy by the inhibition of ubiquitin specific peptidase 10 (USP10) and 13 (USP13) and promote the degradation of class III PI3K complexes through the proteasome pathway (42). Many cancers utilize autophagy as a survival mechanism to maintain viability under stressful conditions (42). Autophagy inhibition was shown to sensitize tumor cells and induce apoptosis under nutritional starvation conditions (42). Interestingly, *Myc* levels decreased with treatment as well (42). We chose to utilize A70 as an alternate combination treatment because of its potential to synergize with rapamycin by preventing autophagy and allowing for rapamycin to down-regulate nutrient receptors and induce cell death in LSCs.

CHAPTER 2: MATERIALS AND METHODS

Mice: *VEC-Cre*$^{+}$*:Pten* $^{loxP/loxP}$*;Rosa*^{floxedSTOP}*;LacZ*$^{+}$ *(Pten null)* T-ALL mice (6,7) and *NOD-SCID-IL2Rγ*$^{-/-}$ (*NSG*) immunodeficient mice were used in this study.

Primary Cells and Cell Lines: Bone marrow, thymocytes, and splenocytes were harvested from *Pten* null T-ALL mice in Hank's Balanced Salt Solution (HBSS) supplemented with 2% Fetal Bovine Serum (FBS), 10mM HEPES, penicillin, and streptomycin to evaluate *in vivo* efficacy of the selected inhibitors. We have recently determined culture conditions that allow for the survival and expansion of primary *Pten* null leukemia cells harvested from primary thymocytes of a *Pten* null mouse with T-ALL. We utilized these cultures as our *in vitro Pten* null T-ALL model. To compare *Pten* null T-ALL to T-ALLs with other genetic lesions, we utilized Jurkat T-lymphoblasts, a human *PTEN* mutant T-ALL cell line that is *NOTCH1* mutant and expresses activated, intracellular domain of NOTCH1 (NICD+). Murine cell lines in this study included: *Kras*WT 12-0 (*Kras* wild type [WT], *Pten* WT [*Pten*+] and activated intracellular domain of NOTCH1 [NICD+]), *Kras*WT 8608 (*Kras* WT, *Pten*+, and NICD+), *Kras*^{G12D} 9r (*Kras* mutant, *Pten*+, NICD+), and TIMI.4 (*Pten*+, NICD+) and were kindly given to our lab from M.Dail at University of California, San Francisco (43). Additional human T-ALL lines included CEM-CCRF T-lymphoblasts (PTEN null, NICD+), MOLT 4 T-lymphoblasts (PTEN null, NICD+), MOLT 3 T-lymphoblasts derived from the same patient as MOLT 4 after relapse (PTEN null, NICD+), and MOLT 16, the human version of our *Pten* null T-ALL, which are *NOTCH1* WT and *PTEN*-deficient. MOLT 16 is an established cell line from a patient with T-ALL and is characterized by a translocation of chromosome 8 (band q24) and chromosome 14 (bandq11) [t(8;14)(q24;qll)] with the

breakpoint mapped to the gene encoding T-cell receptor α-chain (*TCRA*) and the 3' side of *MYC* exons (44). This translocation is analogous to the t(14;15) of our *Pten* null T-ALL model. Human T-ALL cell lines were generously provided by Dr. Genhong Cheng at UCLA (Jurkat), Dr. Caius Radu at UCLA (CCRF-CEM), Dr. Adolfo Ferrando at Columbia University (MOLT-3 and MOLT-4), and Dr. Xiaochun Chen at the University of Maryland (MOLT-16). *Pten* null T-ALL, *Kras*WT 12-0, *Kras*WT 8608, and *Kras*^{G12D} 9r cells were maintained in DMEM supplemented with 20% FBS, 10mM HEPES, non-essential amino acids (NEAA), NaPyruvate, L-glutamine, penicillin, streptomycin, 2-mercaptoethanol (BME), 10ng/mL Interleukin-2 (IL-2), and 10ng/mL Interleukin-7 (IL-7). TIMI.4 were maintained in DMEM supplemented with 10% FBS, penicillin, and streptomycin. Jurkat, CCRF-CEM, MOLT 3, and MOLT 4 lymphoblasts were maintained in RPMI supplemented with 10% FBS, L-glutamine, penicillin, and streptomycin. MOLT 16 lymphoblasts were maintained in RPMI supplemented with 20% FBS, L-glutamine, penicillin, and streptomycin.

Synthetic Agents: Cells were treated with various doses of JQ1, VX-680, Purvalanol A, A70 and/or rapamycin as described in the results section or with appropriate concentrations of dimethyl sulfoxide (DMSO) and ethyl alcohol (EtOH) vehicles. Cells were also treated with the following agents: nocodozale to arrest cells in G_2 or M phase, doxorubicin to inhibit DNA replication in cells, cyclohexamide to prevent protein synthesis, and chloroquine to prevent protein degradation via lysosomes and compared with effects seen by our selected inhibitors. JQ1 was generously provided by James Bradner and A70 was generously provided by J.Yuan (42).

Flow Cytometry: Fluorescence-activated cell sorting (FACS) analysis was performed as

described in previous papers (6-7) with the use of fluors conjugated to antibodies for the following cell surface markers c-Kit, CD71, CD3, CD98, TCRβ, CD45, and IL-7Rα. 7AAD was used for dead cell exclusion. A BD LSRII flow cytometer was used for acquisition of data.

Proliferation and Viability Assays: CellTiter 96 AQ_{ueous} One Solution Cell Proliferation Assay and Vybrant MTT Cell Proliferation Assay modified to accommodate a 24 well plate from the 96 well plate protocol were used to measure viability. Cells were seeded 24hours before drug addition. After 24 and 48 hour incubation in a 5% CO_2 incubator at 37°C with drug or vehicle, MTT or CellTiter 96 AQ_{ueous} One Solution assay reagents were added and absorbance was read at the optical density (OD) specified in assay protocols. BioRad Benchmark microplate spectrophotometer was used for measuring absorbance.

Western Blotting: Cell pellets were lysed in RIPA-lysis buffer and stabilized in 5X sample buffer. Proteins were resolved using SDS-Polyacrylamide Gel Electrophoresis, transferred to PVDF membrane, and probed with phospho-AKT, Phospho-S6 Phospho-Histone H3, LC3B, Phospho-Histone γH2A, PARP, cleaved PARP (c-PARP), caspase3, c-caspase 3, c-Myc, Phospho-c-myc, GAPDH, Aurora B, p53, p21, Glut1, and β-actin antibodies.

Intracellular Staining: Cells were treated with agents, collected at $5x10^6$ cells in 100μL phosphate buffer saline supplemented with 5% FBS, penicillin, and streptomycin (PBS+), stained with cell surface markers, fixed and permeabilized using Invitrogen fix and permeabilization regents, incubated with rabbit polyclonal anti-c-Myc and secondary anti-rabbit Alexa488 antibodies, and then analyzed by FACS.

Standard Giesma cytospin staining: 50,000 -75,000 cells were resuspended in 150µL of PBS+ and cytospun onto glass slides using Thermo Scientific's Cytospin4 at 800rpm for 3 minutes. Giesma staining was performed according to Sigma-Aldrich protocol.

Statistical Analysis

Kaplan-Meier survival curves were utilized to represent animal survival using GraphPad Prism software.

IC_{50} curves were calculated and created using GraphPad Prism software.

CHAPTER 3: COMBINATION DRUG THERAPY IS MORE EFFECTIVE THAN SINGLE INHIBITING AGENTS *IN VIVO.*

The overall purpose of this project was to develop an improved therapeutic treatment for PTEN-deficient T-ALL. Targeting the PI3K/AKT/mTOR pathway with rapamycin was not sufficient to abolish disease; therefore, we attempted to accomplish this objective by co-targeting essential signaling pathways required for LSC formation and *Pten* null T-ALL. Our project consisted of interrogating small molecule inhibitors that target c-Myc through inhibition of bromodomains or reported synthetic lethal interactions, and testing an anti-autophagy small molecule to sensitize T-ALL cells to rapamycin in order to eliminate the disease-initiating population and T-ALL.

Our lab has previously shown *in vivo* that rapamycin treatment significantly reduced the blast population in *Pten* null T-ALL mice; however, rapamycin was unable to eradicate the self-renewing LSC population and eliminate T-ALL (7). We have thus far investigated the ability of VX-680 and JQ1 alone and in combination with rapamycin to eliminate T-ALL *in vivo* using our *Pten* null T-ALL mouse model. For these studies, hematopoietic cells were harvested from primary *Pten* null T-ALL mice and transplanted into *NSG* immuno-compromised recipients for parallel analysis of single and combination agent treatment. Once the *NSG* recipients develop acute disease two to three weeks after transplant, they are treated with drug for 7 or 14 days (Fig.4). Flow cytometry was used to evaluate blast ($CD3^{+}ckit^{-}$) and LSC ($CD3^{+}ckit^{mid}$) compartments in bone marrow after 7 day drug treatments. We found that rapamycin treated mice had decreased blast populations (Fig. 4), however, VX-680 and JQ1 single agent treatment had minimal effects on the blast and LSC populations in treated mice (Fig. 4 and data not shown).

Remarkably, 7 day combination treatment of rapamycin withVX-680 (Fig. 4a, b) and rapamycin with JQ1 treatment (Fig. 4c) caused robust elimination of blasts and more importantly, significantly reduced LSC populations in treated mice.

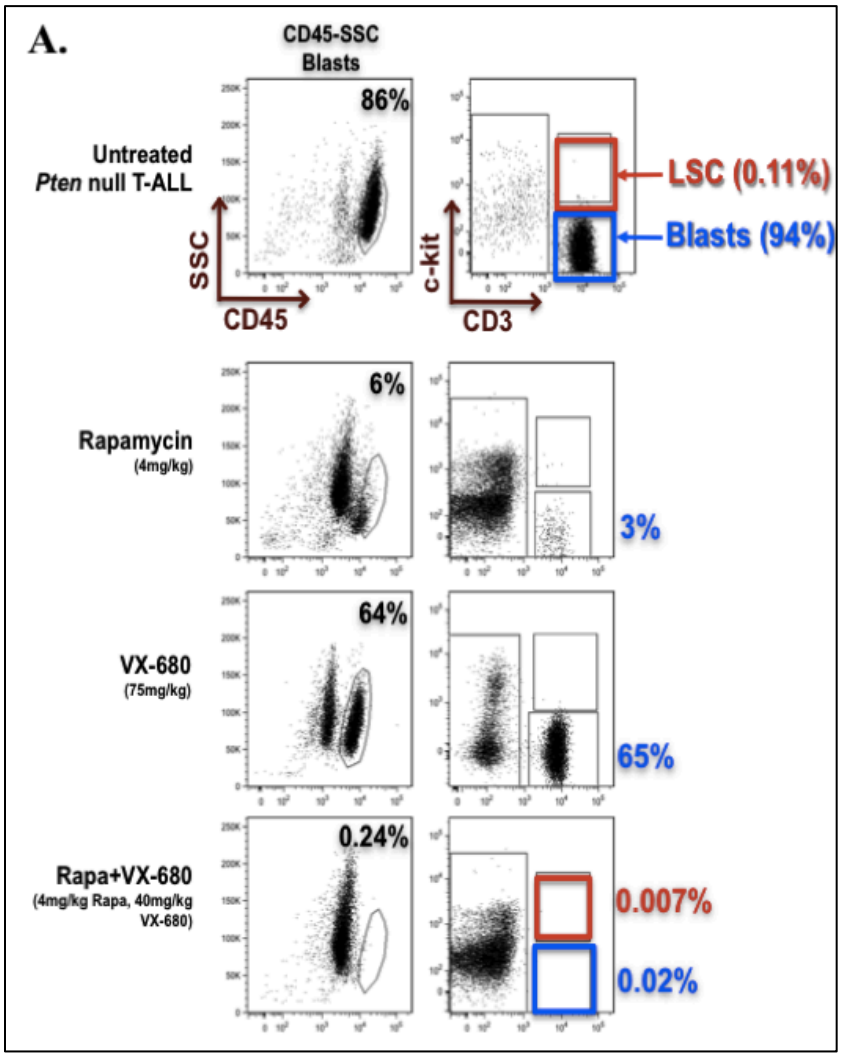

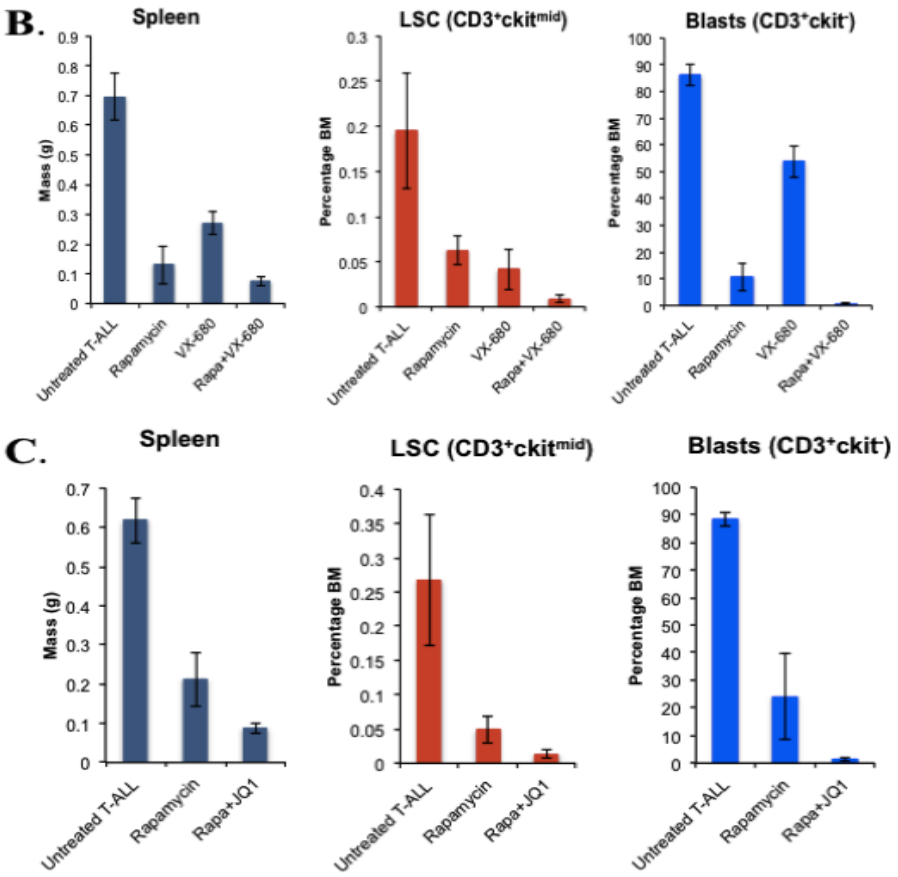

Figure 4: Combination drug therapy is more effective than single inhibiting agents *in vivo.* A.) Combination therapy using rapamycin with VX-680 effectively eliminates blast and LSC populations. FACS analysis of bone marrow harvested from untreated and 7 day rapamycin, VX-680, or rapamycin in combination with VX-680 treatments. B.) Measurement of splenic mass in grams from spleens harvested from *Pten* null T-ALL mice treated with rapamycin, VX-680, or rapamycin in combination with VX-680 for 7 days. Quantitation of percentage of LSC ($CD3^{+}ckit^{mid}$) and blast ($CD3^{+}ckit^{-}$) populations by FACS analysis from bone marrow harvested from *Pten* null T-ALL mice treated with rapamycin, VX-680, or rapamycin in combination with VX-680 for 7 days. C.) Measurement of splenic mass in grams from spleens harvested from *Pten* null T-ALL mice treated with rapamycin or rapamycin in combination with JQ1 for 7 days. Quantitation of percentage of LSC and blast populations by FACS analysis of bone marrow harvested *Pten* null T-ALL mice following 7 day treatment with rapamycin or rapamycin in combination with JQ1.

We performed experiments to functionally test and validate leukemia-initiating cell activity after our single and combination drug treatments. Bone marrow was harvested from untreated, 14 day rapamycin treated, 14 day VX-680 treated, or 14 day rapamycin and VX-680 combination treated mice and transplanted into immuno-compromised *NSG* recipients. Similarly, bone marrow was harvested from 7 day JQ1 treated and 7 day rapamycin and JQ1 combination treated animals and transplanted into immuno-compromised *NSG* recipients. *NSG* mice receiving untreated T-ALL cells succumbed to disease as rapidly as 14 -15 days after transplantation. (Fig.5) Mice transplanted with rapamycin treated cells at cell doses of 10^4 and 10^3 succumbed to disease 25 - 30 days after transplantation and mice transplanted with VX-680 treated cells succumbed 20 - 30 days after transplantation (Fig.5a). Importantly, mice transplanted with bone marrow harvested from animals treated with combination therapy showed significantly greater disease-free survival in comparison to mice transplanted with single agent treated bone marrow (Fig.5). JQ1 single agent treatment on leukemia-initiating activity and survival has not been evaluated nor have the effects of Purvalanol A and A70 as single agents and in combination in our mouse model.

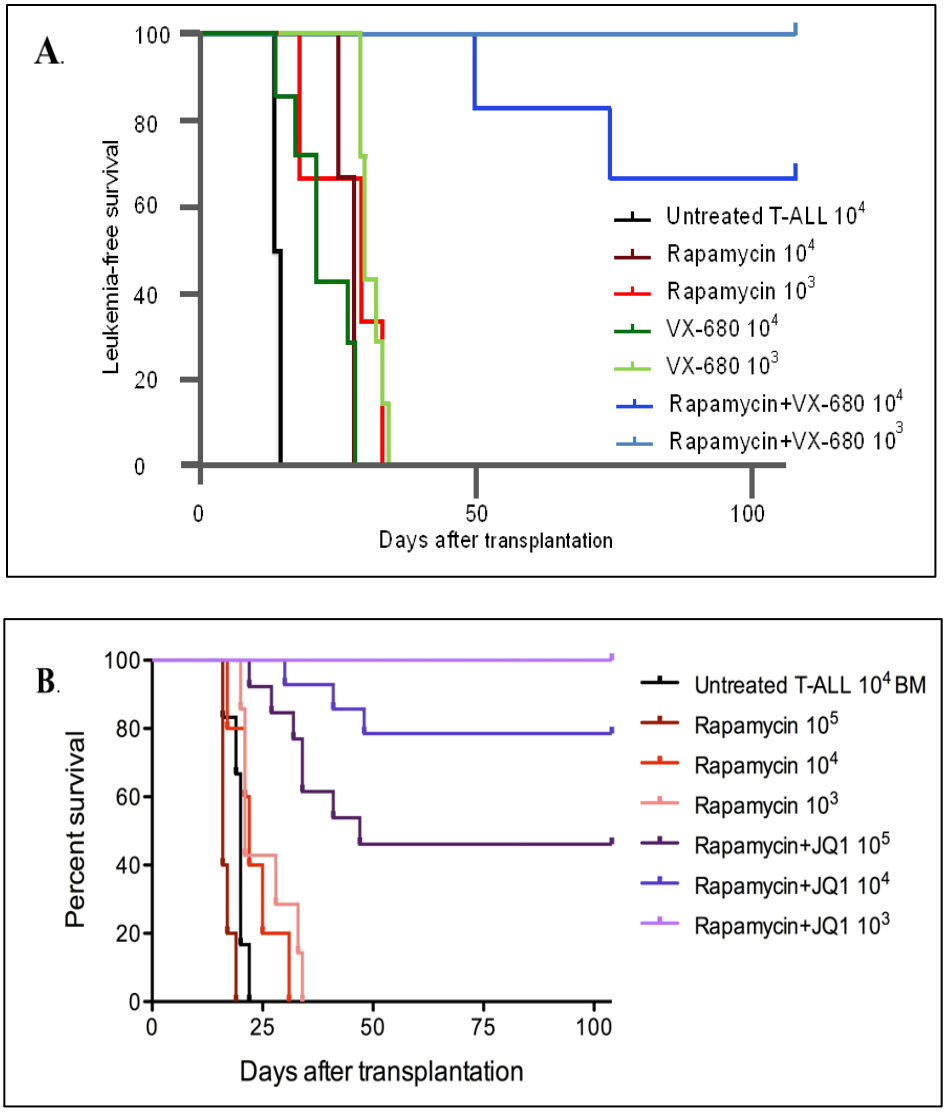

Figure 5: Kaplan-Meier Survival Curves. A.) Rapamycin in combination with VX-680 significantly decreases leukemia-initiating cell activity. Bone marrow was harvested from *Pten* null T-ALL mice after 14 day treatment and transplanted into *NSG* recipients to evaluate leukemia-initiating cell activity. Leukemia-free survival of *NSG* recipients of 10^4 and 10^3 cell doses of treated bone marrow cells. B.) Rapamycin and JQ1 combination treatment effectively reduces LSC activity. Bone marrow was harvested from *Pten* null T-ALL mice after 7 days of treatment and transplanted into *NSG* recipients to evaluate leukemia-initiating cell activity. Leukemia-free survival of *NSG* recipients of 10^5, 10^4, and 10^3 cell doses of treated bone marrow cells.

CHAPTER 4: *PTEN* NULL T-ALL IS SENSITIVE TO SELECTED SMALL MOLECULE INHIBITORS *IN VITRO*.

We screened small molecule inhibitors by performing proliferation and viability assays *in vitro* with our recently generated *Pten* null T-ALL cell line. This culture was derived from primary thymocytes harvested from a *Pten* null mouse with acute T-ALL. After 48 h drug treatment we measured viability to interrogate inhibitor efficacy. Consistent with our previous studies *in vivo*, *Pten* null T-ALL cells were sensitive to rapamycin treatment *in vitro* with significant loss of cell viability at doses as low as 10 nanomolar (nM). Interestingly, viability assays showed our *Pten* null T-ALL cells are sensitive to single agent treatment of VX-680 and JQ1 at nM concentrations as well (Fig. 6). In addition, *Pten* null T-ALL is sensitive to the additive effects of combination VX-680 with rapamycin and JQ1 with rapamycin treatments at nM concentrations (Fig. 6). IC_{50} values of rapamycin, VX-680, and JQ1 were calculated from viability assay data. Concentrations to reduce viability of cell culture population to 50% include 1.148nM of rapamycin, 83.09nM of VX-680, and 250.9nM of JQ1 respectively (Fig. 7).

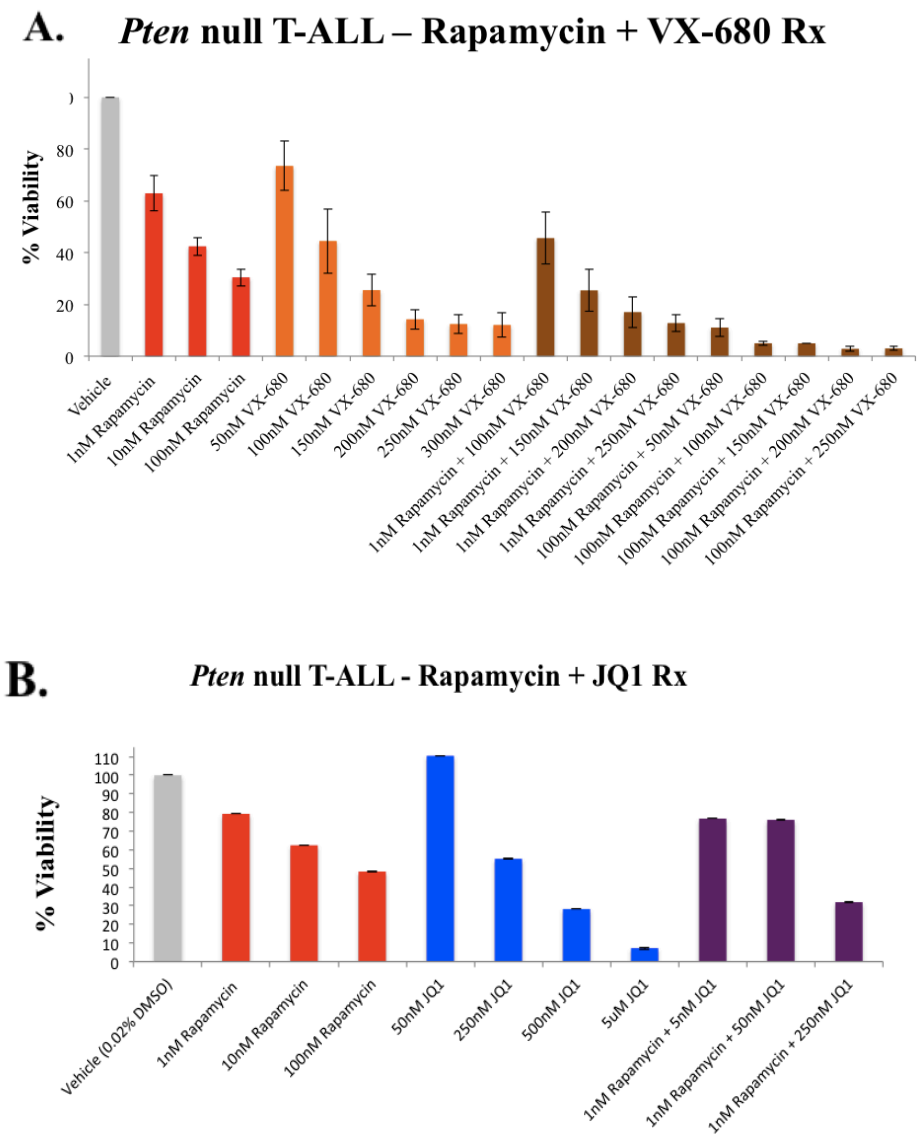

Figure 6: *Pten* null T-ALL rapamycin, VX-680, JQ1, rapamycin with VX-680 and rapamycin with JQ1 combination treated viability assays. A.) Measures percent viability of rapamycin at 1nM, 10nM, and 100nM concentrations (red bars), VX-680 at 50nM, 100nM, 150nM, 200nM, 250nM, and 300nM concentrations (orange bars) as single agents and combination of 1nM, 10nM, and 100nM concentrations of rapamycin with 100nM, 150nM, 200nM, and 250nM concentrations of VX-680 treated (dark orange bars). *Pten* null T-ALL cells relative to vehicle treated *Pten* null T-ALL cells. (0.02% DMSO, grey bar). B.) Measures percent viability of rapamycin at 1nM, 10nM, and 100nM concentrations (red bars), JQ1 at 50nM, 250nM, 500nM, and 5uM concentrations (blue bars) as single agents and combination of 1nM, 10nM, and 100nM concentrations of rapamycin with 5nM, 50nM, and 250nM concentrations of JQ1 treated (purple bars). *Pten* null T-ALL cells relative to vehicle treated *Pten* null T-ALL cells. (0.02% DMSO, grey bar). Cells were seeded in 24-well plates 24h prior to treatment with each drug at varying doses in triplicate and incubated in CO_2 incubators at 37°C for 48h. After 48h, MTT was added to each well and cell viability was measured at O.D.570. Error bars represent standard error.

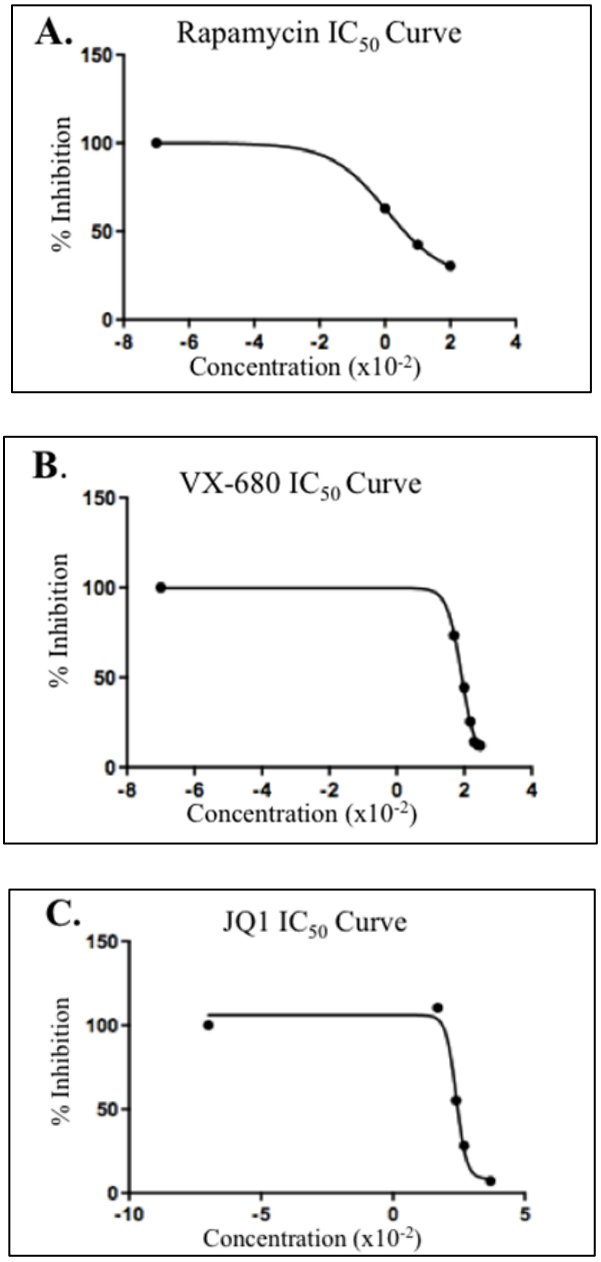

Figure 7: Half maximal inhibitory concentration (IC_{50}) curve values as determined by Graphpad Prism software for treated *Pten* null T-ALL cells. A.) Percent inhibition of rapamycin treated *Pten* null T-ALL cells relative to rapamycin concentrations ranging from1nM to 100nM. B.) Percent inhibition of VX-680 treated *Pten* null T-ALL cells relative to VX-680 concentrations ranging from 50nM to 350nM. C.) Percent inhibition of JQ1 treated *Pten* null T-ALL cells relative to JQ1 concentrations ranging from 5nM to 5µM. *Pten* null T-ALL cells were seeded in 24-well plates 24h before drug addition. Following 48 h incubation in a 5% CO_2 incubator at 37°C with drug or vehicle, 3-2,5-diphenyltetrazolium bromide (MTT) assay reagent was added and measured at optical density (OD) 570nm.

In our viability assays, our *Pten* null T-ALL cells showed sensitivity to A70 at doses as low as 100nM-1μM (Fig.8a). Moreover, sensitivity was observed in rapamycin and A70 dual treated *Pten* null T-ALL cells. Consistent with our hypothesis, A70 appears to synergize with rapamycin to decrease viability following treatment in our *Pten* null cells (Fig.8a). Combination treatment was more effective than single agent rapamycin treatment suggesting A70 may sensitize cells to rapamycin through the inhibition of autophagy. Conversely, combination treatment was not as effective in our viability assays as single agent A70 treatment (Fig. 8a). *Pten* null T-ALL cells showed sensitivity to Purvalanol A at doses as low as 5μM (Fig. 8b). Combination treatments with Purvalanol A have not yet been completed. In contrast to our *Pten* null T-ALL cell line, Jurkat human T-lymphocytes showed very little sensitivity to rapamycin, JQ1, VX-680, and Purvalanol A treatment, even at higher doses (Fig.9). However, Jurkat cells were sensitive to A70 single agent and combination treatments (Fig 9d). Further studies need to be completed to understand the underlying mechanisms of A70 single agent treatment and in combination with rapamycin *in vitro*.

Kras and *NOTCH1* driven murine cell lines were treated with rapamycin, VX-680, and JQ1 and response to inhibitors varied. However, these cell lines were not as sensitive to selected agents as our *Pten* null T-ALL cell line (data not shown). The human T-ALL cell lines MOLT 3, MOLT 4, and CCRF-CEM were also treated with rapamycin, VX-680, JQ1, and Purvalanol A and varied in sensitivity. CCRF-CEM was sensitive to rapamycin, JQ1, and Purvalanol A at higher doses. Unexpectedly, cell viability increased when treated with higher doses of VX-680 (Fig. 10a). VX-680 may not induce apoptosis following polyploidy as seen in our *Pten* null T-ALL cell line or alternative mechanisms

may compensate for Aurora kinase inhibition and allow for continuation through cell cycle progression in these cell lines. However, further evaluation needs to be completed to understand the mechanisms of this resistance. MOLT 4 was not sensitive to any of the inhibitors except for higher doses of JQ1 (Fig. 10b). MOLT 3 was sensitive to JQ1, however, exhibited similar trends to VX-680 treatment of CCRF-CEM and was not sensitive to rapamycin or Purvalanol A treatment (Fig. 10c). MOLT 16 showed sensitivity trends similar to *Pten* null T-ALL when treated with rapamycin, VX-680, JQ1, and Purvalanol A (Fig. 10d). Further viability assays of these cell lines need to be completed and evaluated with more concentrations tested. IC_{50} analysis is essential to complete in order to calculate Purvalanol A and A70 concentrations necessary to reduce cell culture populations to 50% viability and compare inhibitor effects to other T-ALL murine and human cell lines.

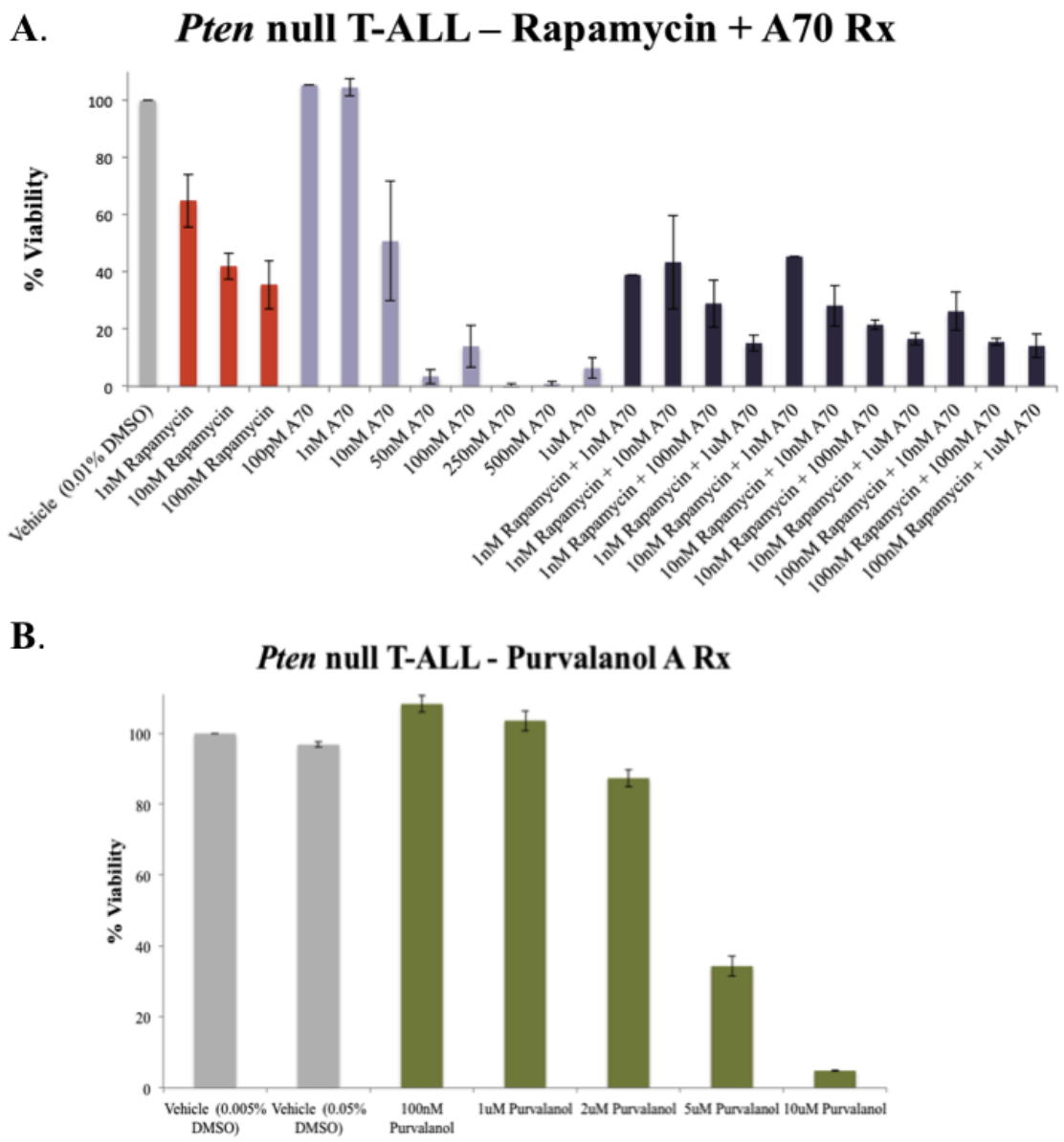

Figure 8: *Pten* null T-ALL A70 and Purvalanol A treated viability assays. A.) Measures percent viability of rapamycin at 1nM, 10nM, and 100nM concentrations (red bars) and A70 at 100pM, 1nM, 10nM, 50nM, 100nM, 250nM, 500nM, and 1uM concentrations (light purple bars) as single agents and in combination of 1nM, 10nM, and 100nM concentrations of rapamycin with 1nM, 10nM, 100nM, and 1uM concentrations of A70 treated (dark purple bars) *Pten* null T-ALL cells relative to vehicle treated *Pten* null T-ALL cells. (.01% DMSO, grey bars). B.) Measures percent viability of Purvalanol A treated *Pten* null T-ALL cells of 100nM, 1μM, 2μM, 5μM, and 10μM concentrations (green bars) relative to vehicle treated *Pten* null T-ALL cells (.005% and .05% DMSO, grey bars). Cells were seeded in 24-well plates 24 h prior to treatment with each drug at varying doses in triplicate and incubated in CO_2 incubators at 37°C for 48h. After 48 h, MTT was added to each well and cell viability was measured at O.D.570. Error bars represent standard error.

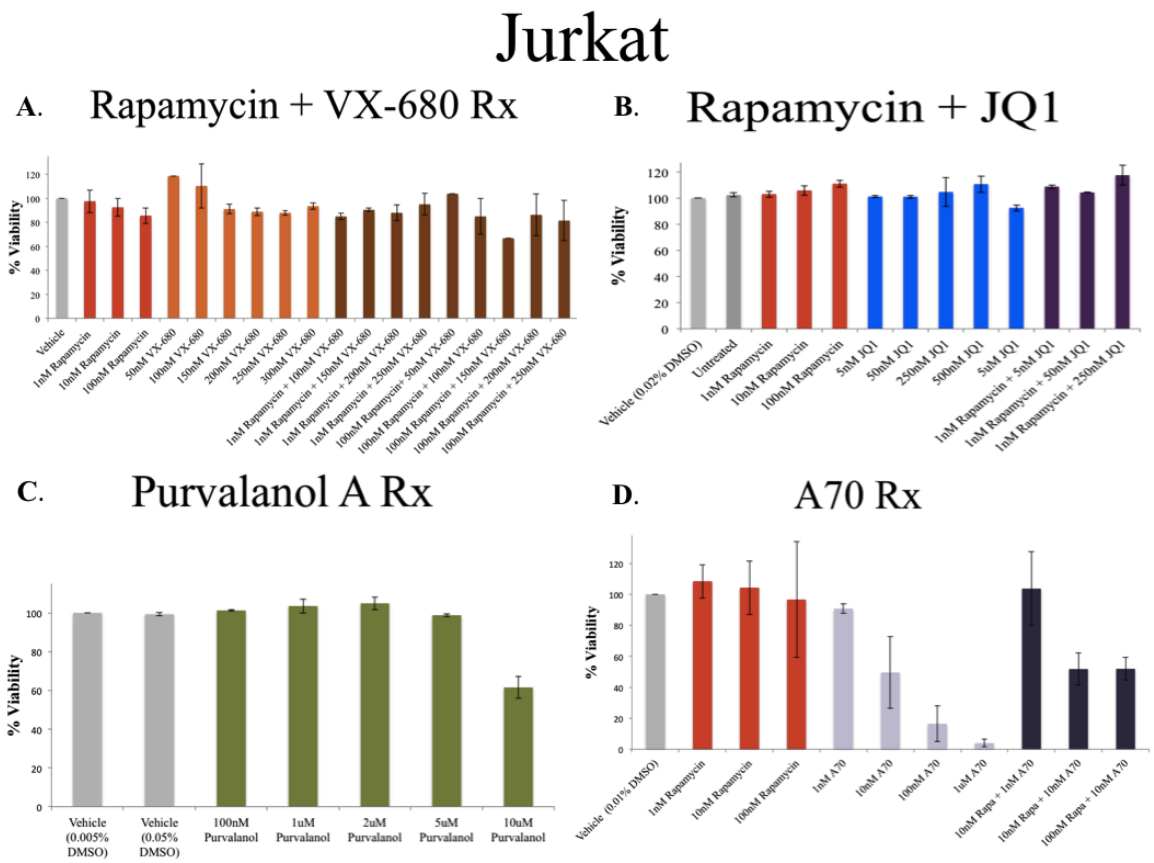

Figure 9: Jurkat single agent and combination treated viability assays. A.) Measures percent viability of rapamycin at 1nM, 10nM, and 100nM concentrations (red bars), VX-680 at 50nM, 100nM, 150nM, 200nM, 250nM, and 300nM concentrations (orange bars) as single agents and combination of 1nM, 10nM, and 100nM concentrations of rapamycin with 100nM, 150nM, 200nM, and 250nM concentrations of VX-680 treated (dark orange bars) Jurkat cells relative to vehicle treated Jurkat cells. (0.02% DMSO, grey bar). B.) Measures percent viability of rapamycin at 1nM, 10nM, and 100nM concentrations (red bars), JQ1 at 50nM, 250nM, 500nM, and 5uM concentrations (blue bars) as single agents and combination of 1nM, 10nM, and 100nM concentrations of rapamycin with 5nM, 50nM, and 250nM concentrations of JQ1 treated (purple bars) Jurkat cells relative to vehicle treated Jurkat cells. (0.02% DMSO, grey bar). C.) Measures percent viability of Purvalanol A treated Jurkat cells of 100nM, 1μM, 2μM, 5μM, and 10μM concentrations (green bars) relative to vehicle treated Jurkat cells (.005% and .05% DMSO, grey bars). D.) Measures percent viability of A70 at 100pM, 1nM, 10nM, 50nM, 100nM, 250nM, 500nM, and 1uM concentrations (light purple bars) as single agents and in combination of 1nM, 10nM, and 100nM concentrations of rapamycin with 1nM, 10nM, 100nM, and 1uM concentrations of A70 treated (dark purple bars) Jurkat cells relative to vehicle treated Jurkat cells (.01% DMSO, grey bars). Cells were seeded in 24-well plates 24h prior to treatment with each drug at varying doses in triplicate and incubated in CO_2 incubators at 37°C for 48h. After 48h, MTT was added to each well and cell viability was measured at O.D.570. Error bars represent standard error.

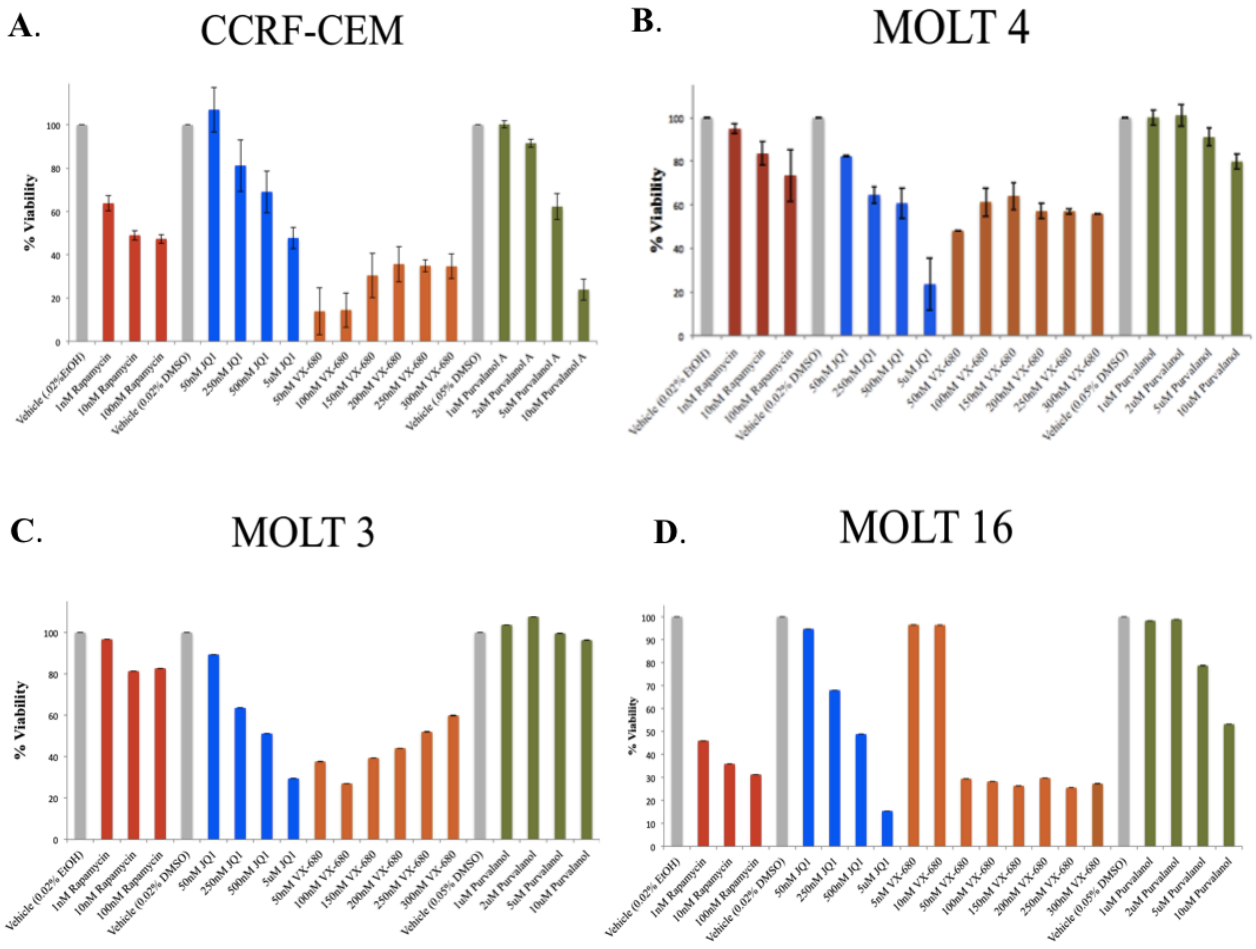

Figure 10. Single agent treated Human T-ALL viability assays. Measures percent viability of rapamycin at 1nM, 10nM, and 100nM concentrations (red bars), JQ1 at 50nM, 250nM, 50nM, and 5uM (blue bars), VX-680 at 5nM, 50nM, 100nM, 150nM, 200nM, 250nM, and 300nM (orange bars), and Purvalanol A at 1uM, 2uM, 5uM, and 10uM (green bars). Human T-ALL cells relative to vehicle treated T-ALL cells. (.01% EtOH, .01% DMSO, and .05% DMSO, grey bars) A.) CCRF-CEM cell line B.) MOLT 3 cell line C.) MOLT 4 cell line D.) MOLT 16 cell line. Cells were seeded in 24-well plates 24h prior to treatment with each drug at varying doses in triplicate and incubated in CO_2 incubators at 37°C for 48h. After 48h, MTT was added to each well and cell viability was measured at O.D.570. Error bars represent standard error.

We utilized our recently derived *Pten* null T-ALL cell line in order to understand the molecular and cellular mechanisms underlying single agent treatment and decreased cell viability observed in our viability assays. Propidium iodide staining and flow cytometry was completed to assess the effects of rapamycin and VX-680 on cell cycle. Rapamycin treated *Pten* null T-ALL cells were observed to accumulate at the G_0/G_1 stage suggesting G_1 arrest following 12 h of treatment (Fig. 11). VX-680 has been shown to block mitosis, prevent cytokinesis, and cause polyploidy through inhibition of Aurora kinases, which are known to be essential for cell cycle progression and cytokinesis (29). We found that VX-680 treatment did not prevent DNA synthesis in our *Pten* null T-ALL cells (Fig. 12). VX-680 caused accumulation of treated cells in G_2/M stage, formation of a >4N population, and led to a robust increase in sub G_0/G_1 apoptotic population following 4-24 h treatment (Fig.12). Morphologically, this can be seen with Giemsa stained samples of *Pten* null T-ALL cells treated with 300nM VX-680 for 24 h in comparison to 0.02% DMSO vehicle treated cells (Fig.13a). Following 24 h VX-680 treatment, extensive death of *Pten* null T-ALL cells can be seen compared to 24h vehicle treatment (Fig.13a). In contrast to *Pten* null T-ALL cells, apoptosis was not observed in Jurkat cells following 24h 300nM VX-680 treatment (Fig. 13b,c). However, VX-680 caused polyploidy in Jurkat cells resulting in >8N populations after 48 h and 72 h treatment (data not shown).

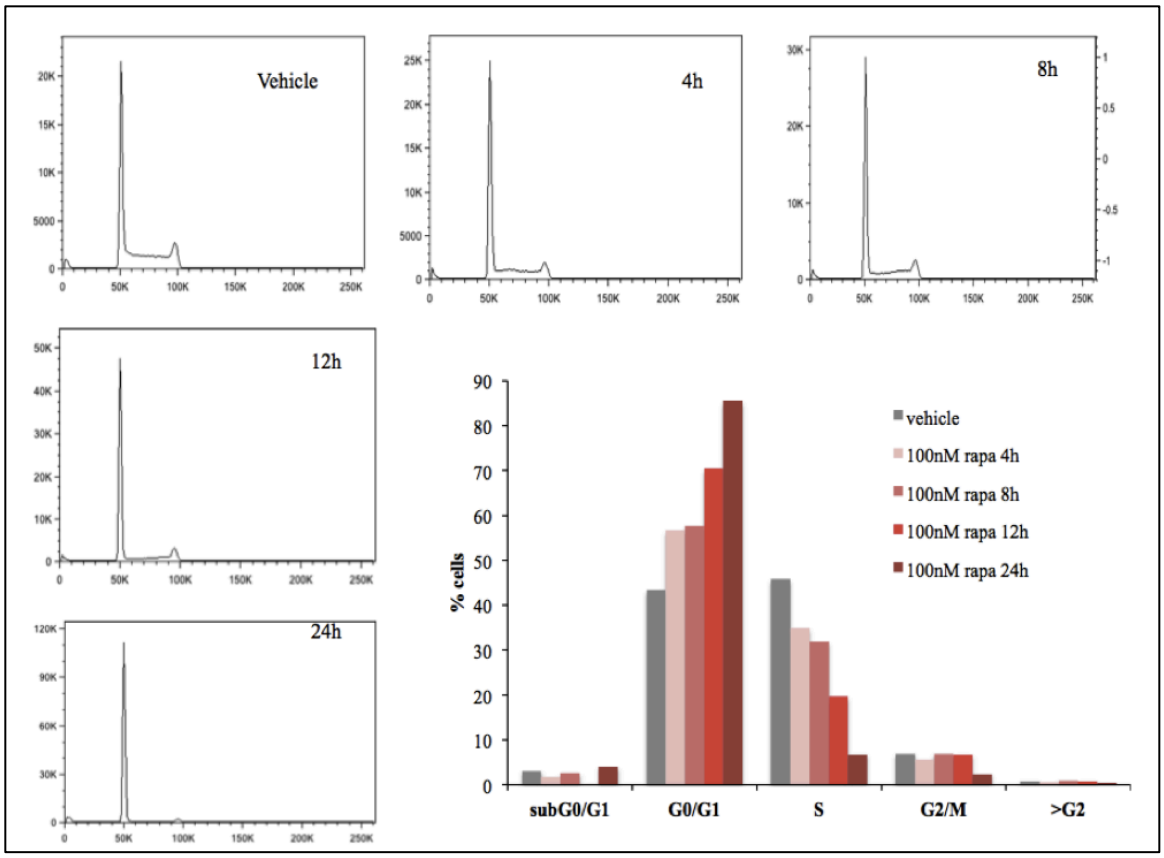

Figure 11: Propidium iodide staining, cell cycle analysis by FACS, and quantification of vehicle (.02% EtOH) and 100nM rapamycin effects on *Pten* null T-ALL. Bar graphs represent percent of cells of vehicle (gray bars), 4 h 100nM rapamycin (pink bars), 8 h 100nM rapamycin (light red bars), 12 h 100nM rapamycin (red bars), and 24 h 100nM rapamycin (dark red bars) treatment in subG_0/G_1, G_0/G_1, S, G_2/M, and >G_2 portions of the cell cycle. *Pten* null T-ALL cells were seeded on 10cm plates 24 h prior to treatment and collected at indicated treatment times.

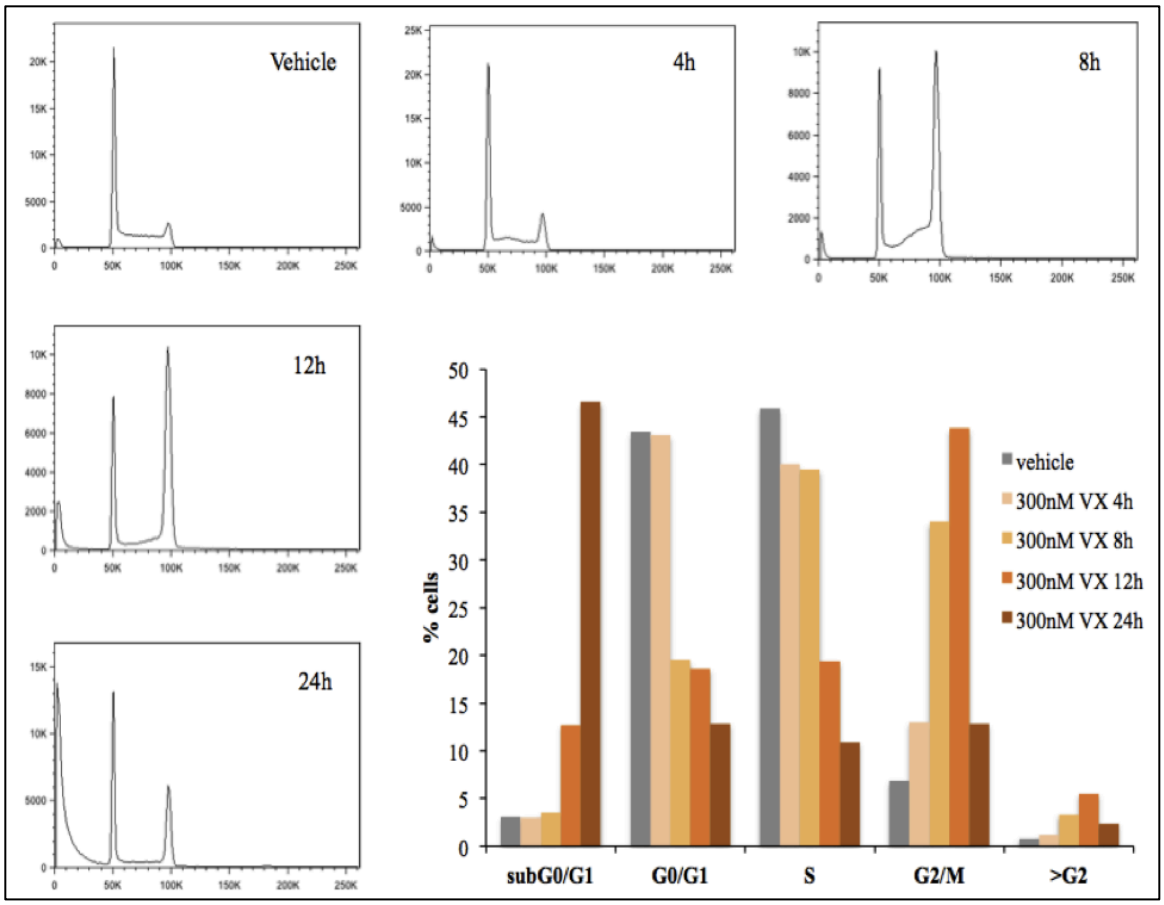

Figure 12: Propidium iodide staining, cell cycle analysis by FACS, and quantification of vehicle (.02% DMSO) and 300nM VX-680 effects on *Pten* null T-ALL. Bar graphs represent percent of cells of vehicle (gray bars), 4 h 300nM VX-680 (peach bars), 8 h 300nM VX-680 (light orange bars), 12 h 300nM VX-680 (orange bars), and 24 h 300nM VX-680 (dark orange bars treatment in subG_0/G_1, G_0/G_1, S, G_2/M, and >G2 portions of the cell cycle. *Pten* null T-ALL cells were seeded on 10cm plates 24 h prior to treatment and collected at indicated treatment times.

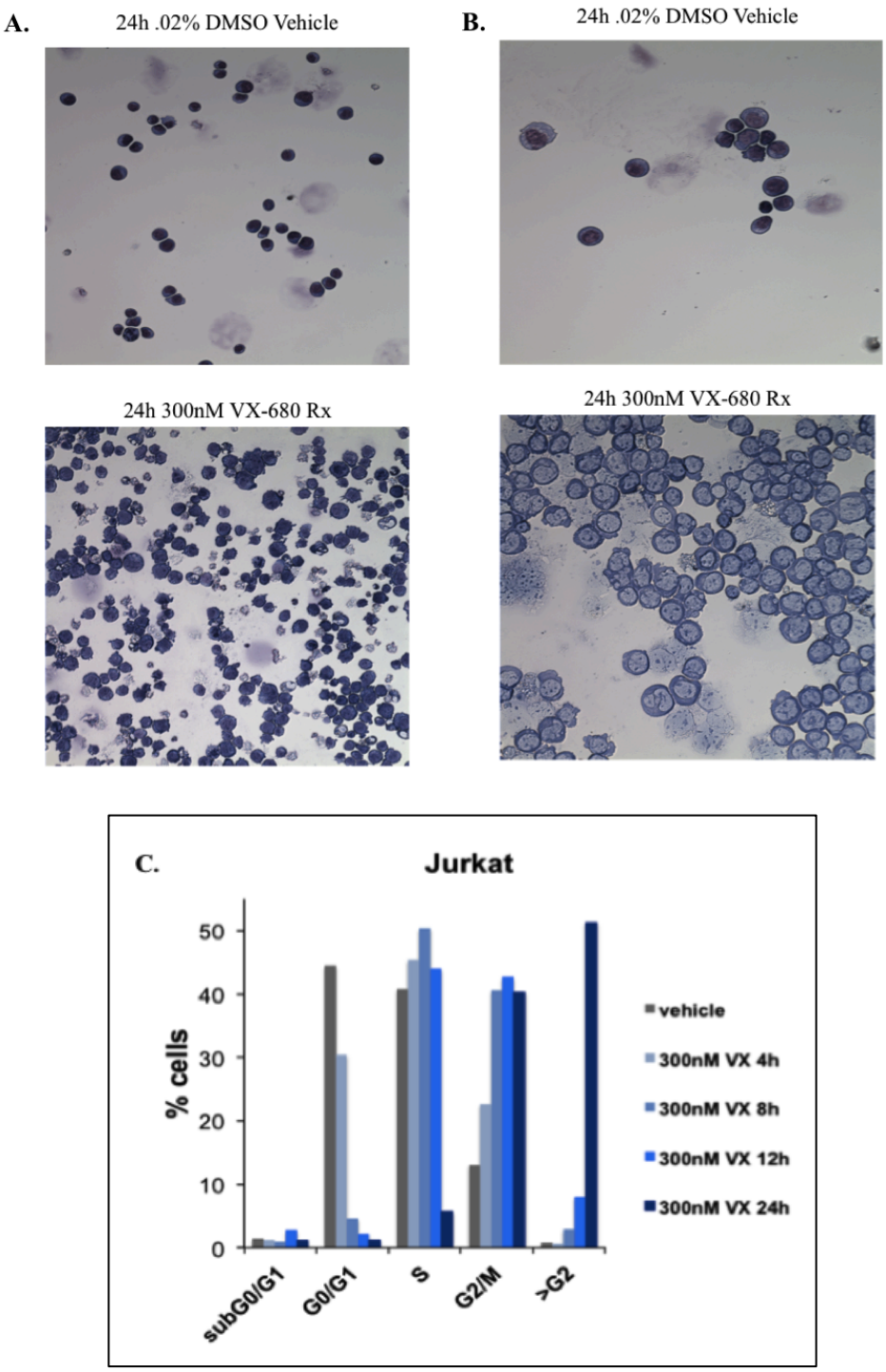

Figure 13: Standard Giesma cytospin staining of 24h vehicle (.02% DMSO) and 24h 300nM VX-680 treated cells. A.) *Pten* null T-ALL cells at 200x magnification. B.) Jurkat cells at 200x magnification. The stained cells were observed under a light microscope. C.) Quantitation of cell cycle analysis using propidium iodide staining in Jurkat cells. Bar graphs represent percent of vehicle (gray bars), 4 h 300nM VX-680 (light blue bars), 8 h 300nM VX-680 (blue bars), 12h 300nM VX-680 (royal blue bars), and 24 h 300nM VX-680 (dark blue bars) treated cells in subG_0/G_1, G_0/G_1, S, G_2/M, and >G2 portions of the cell cycle.

CD71 and CD98 are essential for nutrient uptake during thymocyte differentiation and expressed during immature thymocyte proliferation. CD71 is the transferrin receptor, essential for cellular uptake of iron and cell growth (45). CD98, an amino acid transporter subunit, is involved in cell activation and calcium flux events. Interestingly, we found that *Pten* null T-ALL blasts were highly sensitive to the down-regulation of these nutrient receptors following 24 h rapamycin treatment. However, *Pten* null T-ALL LSCs were resistant to the down-regulation of these receptors (Fig.14), consistent with our previous studies (7). LSC lack of response to single agent rapamycin treatment in contrast to blasts may be due to intrinsic mechanisms specific to LSCs that is protective to rapamycin effects on nutrient receptors. This supports our concept of utilizing combination treatment to eliminate both blasts and LSCs as an improved treatment since rapamycin alone is insufficient to eliminate *Pten* null T-ALL LSCs. Similar to *Pten* null T-ALL LSCs, Jurkat cells did not show down-regulation of nutrient receptors after 24 h rapamycin treatment (data not shown). It has been difficult to evaluate nutrient receptor expression in our *Pten* null T-ALL mouse model *in vivo*. This may be due to rapid cell death and clearing of treated cells.

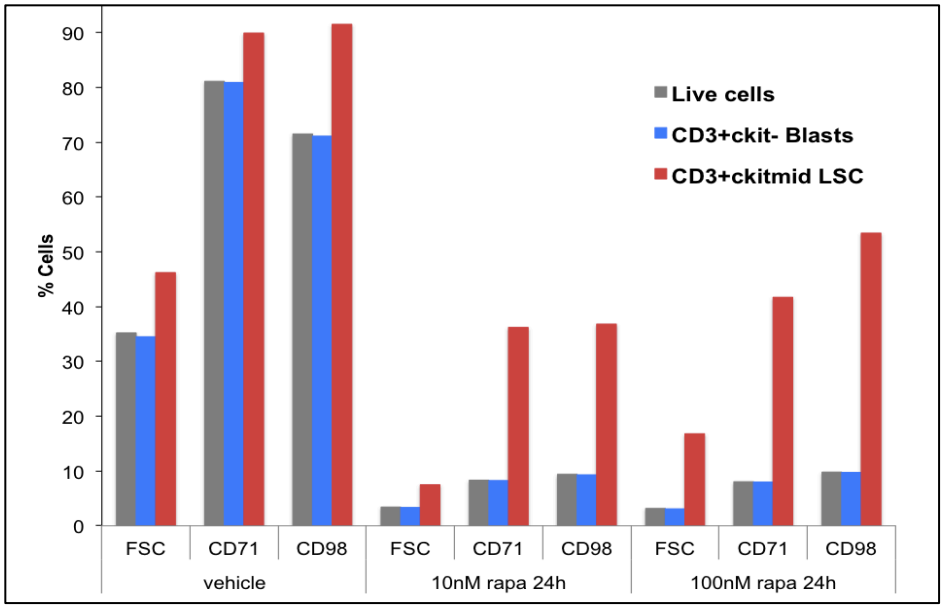

Figure 14: *Pten* null T-ALL LSC are resistant to down-regulation of nutrient receptors by rapamycin *in vitro.* Graph represents quantitation of cell size, CD71, and CD98 in populations of live cells (gray bars), blasts ($CD3^{+}ckit^{-}$, blue bars), and LSCs ($CD3^{+}ckit^{mid}$, red bars) after vehicle (.02% EtOH), 10nM rapamcyin, and 100nM rapamycin treatment for 24 h. Cells were treated with agents, stained with cell surface markers including nutrient receptor markers CD71 and CD98, T-cell specific markers CD3 and c-kit, and analyzed by FACS. 7AAD was used for dead cell exclusion.

Since c-Myc has been reported to transcriptionally activate CD71 expression (45), we investigated whether JQ1 treatment would cause down-regulation of this receptor in our *Pten* null T-ALL cells. Robust down-regulation of CD71 was observed beginning at 12 h with 500nM JQ1 treatment in *Pten* null T-ALL (Fig.15). Additionally, JQ1 has been shown to down-regulate *Myc* expression, bind to *cis* elements in the *IL-7R* promoter, and suppress *IL-7R* expression (33-38). Our *Pten* null cell line has been shown to overexpress *Myc* and requires IL-7 enriched media. Therefore, we investigated whether these cells were sensitive to JQ1 inhibitory effects. To examine if JQ1 down-regulates levels of Myc and the IL-7 receptor, we treated *Pten* null T-ALL and Jurkat cells 24 h with a dose range of JQ1 for 24 h, used FACS to evaluate surface expression levels of IL-7Rα, and used intracellular straining to measure Myc levels within the cells. (Fig. 15,16)

JQ1 down-regulated Myc following 12 h 500nM treatment. JQ1 caused robust down-regulation of IL-7Rα levels as early as 3 h of 500nM JQ1 treatment and at doses as low as 250nM following 24 h treatment in *Pten* null T-ALL (Fig.15). Interestingly, the majority of the *Pten* null T-ALL population, the blast compartment, was sensitive to JQ1 down-regulation of IL-7α; however, the *Pten* null T-ALL LSC population was resistant to down-regulation of IL-7Rα (data not shown). IL-7Rα is important for preventing apoptosis during differentiation of thymocytes (37). *Pten* null LSC resistance and differential response to JQ1 mediated IL-7Rα down-regulation may be caused by a differential response to utilize alternative mechanisms to counter the down-regulation IL-7Rα and maintain survival. In contrast, we found LSCs are substantially more sensitive to down-regulation of c-Myc by JQ1 treatment than the blast compartment (Fig. 16). This may be due to different regulation of bromodomains and their c-Myc recruitment to genes in LSCs and blast compartments.

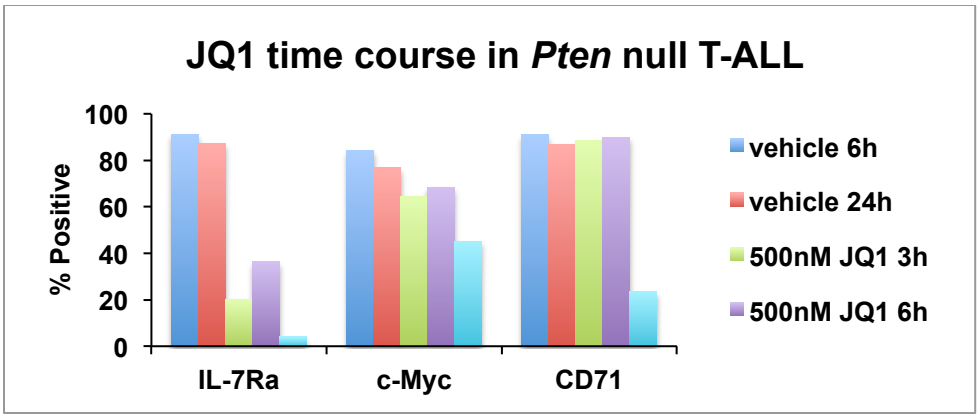

Figure 15: JQ1 down-regulates IL-7Rα, c-Myc, and CD71 levels in *Pten* null T-ALL cells. Measurement of percent positive IL-7Rα, c-Myc, and CD71 surface expression in *Pten* null T-ALL cells following vehicle treatment (.01% DMSO, 6 h - blue bars, 24 h - red bars), 3 h 500nM JQ1 treatment (green bars), 6 h 500nM JQ1 treatment (purple bars), and 12 h 500nM JQ1 treatment (light blue bars) by FACS analysis. Cells were treated with inhibiting agent and collected at various time points, stained with cell surface markers, and analyzed by FACS. To investigate intracellular c-Myc regulation, cells were fixed and permeabilized using Invitrogen fix and permeabilization regents, incubated with rabbit polyclonal anti-c-Myc and secondary antibodies, and then analyzed by FACS.

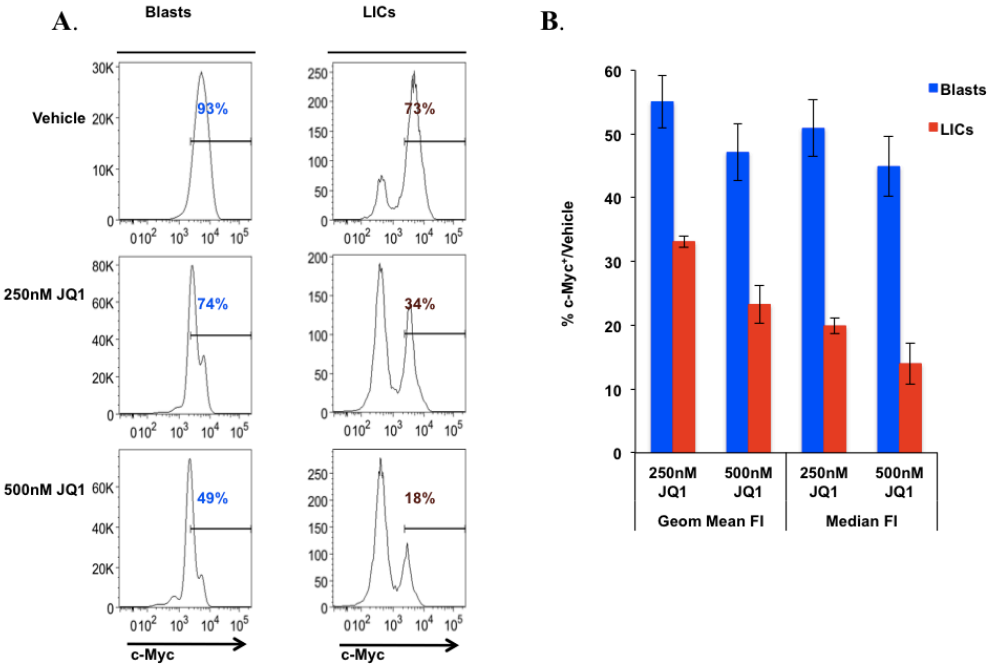

Figure 16: *Pten* null T-ALL blasts and LSCs respond differently to JQ1 treatment. A.) Representative FACS histogram plots showing the frequency of Myc$^+$ cells in blast and LSC populations in *Pten* null T-ALL after 24 hour JQ1 treatment. B.) Quantitation of geometric mean and median flourescence intensities of c-Myc using flow cytometric analysis after 24 hour JQ1 treatment.

CHAPTER 5: CHARACTERIZING BIOCHEMICAL MECHANISMS UNDERLYING EFFICACY OF SELECTED INHIBITORS.

We completed Western blots to investigate biochemical signaling pathway response to our selected inhibitors. We investigated if the inhibitory drugs are reaching the intended target by looking at known downstream targets and evaluated effects of selected small molecule inhibitors by identifying markers that indicate induction of certain pathways such as apoptosis. *Pten* null T-ALL and Jurkat cells were treated with a range of doses of rapamycin, VX-680, JQ1, and nocodozale followed by collection over a 4-24 h-time course for biochemical analysis. As expected, Western blots revealed rapamycin treated *Pten* null T-ALL cells have decreased levels of phospho-S6, a downstream target of the mTOR pathway (Fig. 17a). VX-680 treatment decreased phospho-histone H3 levels, the downstream target of Aurora kinases and induced levels of phospho-histone γH2A, an indication of DNA damage response. VX-680 treatment also resulted in increased levels of cleaved caspase 3 and cleaved PARP, consistent with apoptosis (Fig. 17a). Interestingly, VX-680 did not appear to activate apoptosis pathways in Jurkat cells, consistent with our cell cycle analysis data where we see polyploidy but no increased accumulation in sub G_1 population. 24h JQ1 treatment causes down-regulation of c-Myc and phospho-c-Myc in *Pten* null T-ALL cells at doses as low as 250nM (Fig. 17b). Induction of apoptosis by JQ1 was also observed by increased levels of cleaved caspase 3 and cleaved PARP (Fig.17b). Jurkat cells were less sensitive to c-Myc down-regulation by JQ1 and did not show induction of apoptosis (Fig.17c). It has been previously reported Aurora kinases A and B are up-regulated by Myc and are essential for maintenance of the malignant state (29). Our Western data revealed that

down-regulation of c-Myc by JQ1 in *Pten* null T-ALL cells correlated with the down-regulation of Aurora B and this down-regulation may contribute to the cellular effects of JQ1 treatment (Fig.17d). Down-regulation of Aurora B was not observed in JQ1 treated Jurkat cells (Fig.17d).

A. ***Pten* null T-ALL**

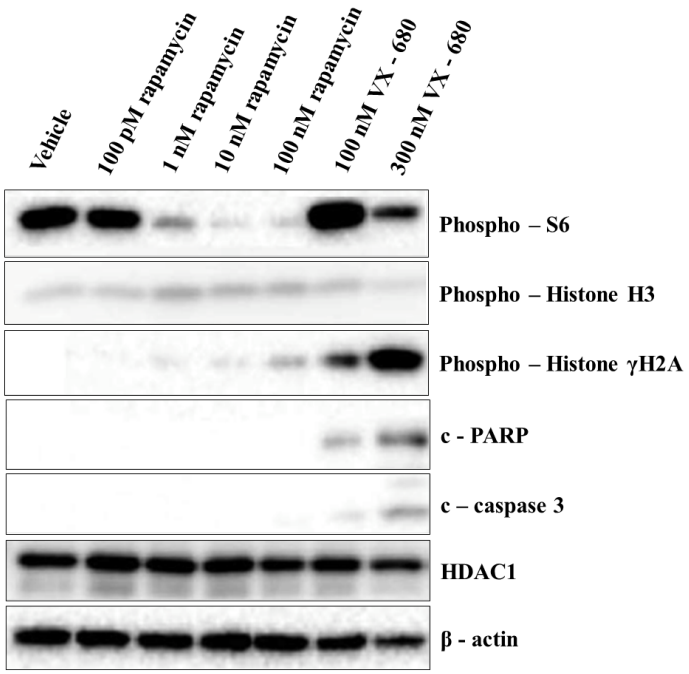

B. ***Pten* null T-ALL**

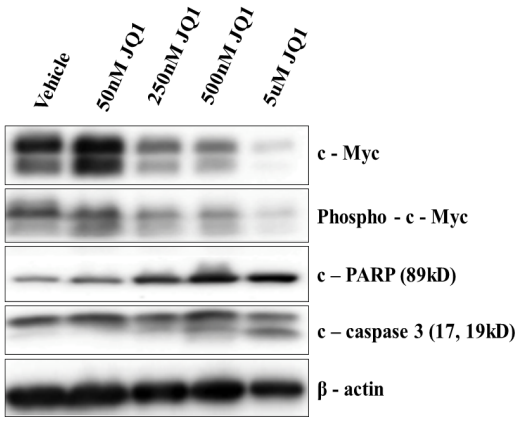

C. **Jurkat**

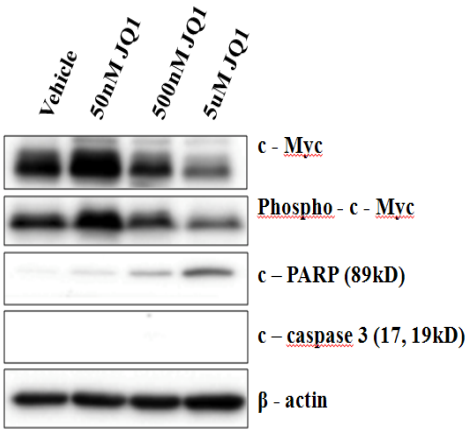

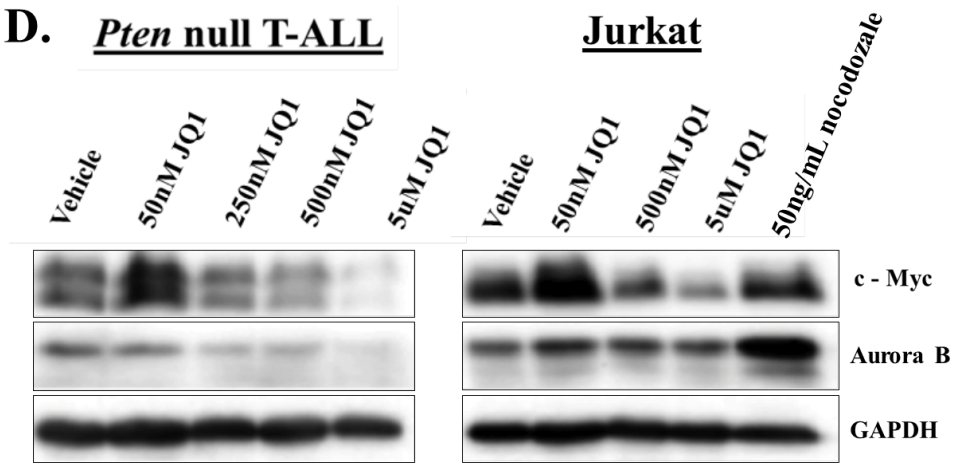

Figure 16: Biochemical analysis of signaling pathway response and mechanisms of selected inhibitors on apoptosis, autophagy, and known downstream target markers by Western blot. A.) Examination of vehicle (.02% DMSO), 100pM rapamycin, 1nM rapamycin, 10nM rapamycin, 100nM rapamcyin, 100nM VX-680, and 300nM VX-680 treatment effects on the phosphorylation of S6, Histone H3, and Histone γH2A, or cleavage of PARP and caspase 3 in *Pten* null T-ALL cells. B.) Examination of vehicle (.02% DMSO), 50nM JQ1, 250nM JQ1, 500nM JQ1, and 5uM JQ1 treatment effects on cMyc, the phosphorylation of cMyc, and cleavage of PARP and caspase 3 on *Pten* null T-ALL cells. C.) Examination of vehicle (.02% DMSO), 50nM JQ1, 250nM JQ1, 500nM JQ1, and 5uM JQ1 treatment effects on c-Myc, the phosphorylation of c-Myc, and cleavage of PARP and caspase 3 on Jurkat cells. D.) Examination of Myc and Aurora B levels in *Pten* null T-ALL and Jurkat cells in response to vehicle (.02% DMSO), 50nM JQ1, 500nM JQ1, and 5uM JQ1 treatment and 50ng/mL nocodozale treatment. HDAC, β-actin, and GAPDH were utilized as loading controls.

CHAPTER 6: DISCUSSION

In this study, we interrogated small molecule inhibitors to investigate targeted combination treatment as an approach to eradicate blasts and more importantly, LSCs to eliminate *Pten* null T-ALL in our genetic mouse model and derived cell lines. We found *Pten* null T-ALL is sensitive to dual treatment and *Pten* null T-ALL LSCs respond differently to treatments compared to differentiated blasts. Furthermore, we identified underlying mechanisms of drug efficacy of small molecule inhibitors on *Pten* null T-ALL. Our data suggests co-targeting of the PI3K/AKT/mTOR pathway and Myc overexpression from chromosomal translocation is an effective strategy to eliminate both the bulk of the disease consisting of blasts and the cycling and proliferating LSCs in *Pten* null T-ALL.

Our quantitative and functional assays demonstrated *Pten* null T-ALL mice are not as sensitive to single agent treatment of selected small molecule inhibitors rapamycin, VX-680, and JQ1 as they are to combination treatments. *Pten* null T-ALL mice treated with rapamycin as a single agent showed prolonged survival however, rapamycin cannot eliminate LSCs and does not cure T-ALL as shown in Guo et. al. (2011). Similarly, VX-680 and JQ1 as single agents are unable to eliminate LSCs as seen with transplantation into NSG mice. However, combination drug therapy of rapamycin with VX-680 and rapamycin with JQ1 effectively eliminates blast and more importantly, significantly decreased LSC populations supporting the quantitative decrease observed in our FACS analysis.

Cell viability assays showed our *Pten* null T-ALL cell line is sensitive to selected inhibitors VX-680, JQ1, Purvalanol A, and A70 as single agents. Furthermore, VX-680

and JQ1 in combination with rapamycin were observed to have an additive effect on our *Pten* null T-ALL cells whereas A70 in combination with rapamycin had a synergistic effect. Our studies demonstrate a more robust effect with dual treatment in our *in vivo* and *in vitro* models compared to single agent rapamycin, VX-680, and JQ1 therapy, reaffirming our hypothesis of co-targeting essential pathways by combination drug treatment as a potential, improved form of drug therapy for PTEN-deficient T-ALL. It is important to further evaluate Purvalanol A and A70 efficacy *in vivo* as single agents and in combination with rapamycin. We would like to determine if Purvalanol A and A70 are tolerated in mice and whether these agents are effective alone and in combination with rapamycin in our mouse model since our *Pten* null T-ALL cell line was sensitive to Purvalanol A and A70 treatments *in vitro*. We also would like to characterize their biochemical mechanisms of inhibitory effects utilizing our *Pten* null T-ALL cell line.

Molecular, biochemical, and cellular analysis revealed mechanisms underlying efficacy of rapamycin, VX-680, and JQ1 as single agents and in combination. In our study, we found rapamycin caused accumulation of cells in G_0/G_1 stage, suggestive of a G_1 arrest and may be due to the down-regulation of nutrient receptors, CD71 and CD98 observed in our *Pten* null T-ALL cells. Sensitivity to blocked nutrient uptake following 24 h rapamycin treatment may contribute to the mechanism by which rapamycin eradicates blasts, however, LSCs are less sensitive to the down-regulation of nutrient receptors. LSC resistance to rapamycin treatment has been proposed to be due to the inability of rapamycin to affect mTOR signaling in these cells (7). Autophagy is a catabolic process cancer cells have been shown to utilize as a mechanism for the cell to continue to thrive under nutrient poor conditions (42). We propose a potential therapy to

eradicate these rapamycin resistant LSC would be to dual treat these cells with the anti-autophagy agent, A70, to sensitize these cells by promoting the degradation of class III PI3K and down-regulate Myc expression as seen in studies by Liu (2011) in combination with rapamycin. However, further studies still need to be completed such as quantifying efficacy of A70 as a single agent and in combination *in vivo*, identification of a presence or absence of LC3 induction, an indicator for autophagy, and assessment of Myc levels using biochemical analyses.

Inhibition of Aurora A has been shown to disrupt cell cycle progression and inactivity of Aurora B has been shown to prevent cytokinesis and lead to polyploidy in tumor cells (29). In our *Pten* null T-ALL cells, we found VX-680 causes a block in mitosis but does not block DNA synthesis. We observed an accumulation of cells in G_2/M of the cycle and a formation of >4N population with an increased apoptotic (subG_0/G_1) population. Our data suggests that VX-680 treatment is synthetic lethal in our *Myc* overexpressing *Pten* null T-ALL LSCs, similar to responses of cells overexpressing Myc treated with VX-680 in Yang et. al. (2010). Interestingly, our *Pten* null LSCs are actively cycling, in contrast to most LSCs in other hematopoietic malignancies such as acute myelogeneous and chronic myelogenous where LSCs reside mostly in a quiescent state (11). This actively cycling state may be the reason LSCs are especially sensitive to VX-680's effect on cell cycle. Biochemical analysis reveals VX-680 reduces levels of the known down-stream target of Aurora kinases, phospho-histone H3, induces levels of phospho-histone γH2A, and increased levels of cleaved caspase 3 and cleaved PARP, consistent with apoptosis and apoptotic (subG_0/G_1) population seen in our cell cycle analysis and in studies by Harrington et. al. (2004) and Yang et. al. (2010).

In our *Pten* null T-ALL blast population, JQ1was shown to down-regulate Myc with subsequent down-regulation of CD71 and IL-7Rα levels as seen in our FACS analysis. Our results are consistent with studies by O'Donnell et. al. (2005) and Ott (2012) which show CD71 and IL-7Rα are regulated by Myc expression. However, the *Pten* null T-ALL LSC population was found to be resistant to IL-7Rα down-regulation. The enhanced sensitivity of *Pten* null T-ALL LSCs to Myc down-regulation by JQ1 may be particularly valuable to efficiently target *Pten* null T-ALL LSCs with deregulated Myc to eliminate these cells. Taken together, our study shows that LSC and blast subpopulations are not only functionally distinct but respond differently to targeted treatments and are both sensitive to JQ1 treatment through different mechanisms. Biochemical analysis reveals JQ1 treatment caused down-regulation of c-Myc, phospho-c-Myc, and Aurora B expression in *Pten* null T-ALL cells, and induction of apoptosis as indicated by increased levels of cleaved caspase 3 and cleaved PARP. c-Myc expression levels correlated with Aurora B expression similar to the observations from the study by Hollander et.al. (2010) in B-cell lymphoma.

In comparison, Jurkat cells were not sensitive to selected inhibitors, the down-regulation of nutrient receptors by rapamycin, and were less sensitive to c-Myc down-regulation by JQ1 *in vitro.* Our data suggests the role of nutrient receptors may be different in Jurkat cells and they may not be as dependent on these nutrient receptors as our *Pten* null T-ALL blast population. Interestingly, VX-680 did not appear to activate apoptotic pathways in Jurkat cells, consistent with our cell cycle analysis data where we see polyploidy but no increased accumulation in sub G_1. Jurkats were not sensitive to JQ1 as seen in our viability assays, FACS analysis, and Western blots which is consistent with

what was observed in Zuber et. al. (2011). Additionally, JQ1 treatment does not induce apoptosis in Jurkats in contrast to our *Pten* null T-ALL cells.

Since LSCs respond differently to targeted therapies, we would like to further investigate if there is a resistant response to treatment and if so, the mechanisms of resistance by examination of mice that initially respond to our single agent and proposed combination therapy but relapse and succumb to disease as seen in single agent rapamycin treatment. Studies suggest CSCs may be resistant to current therapies due to intrinsic differences that may be protective to these cells (11). It is important to identify these populations and their underlying mechanisms of resistance to put forth effective therapies. Relapse can potentially be attributed to the addition of new lesions in our LSCs or emergence of a genetically distinct and different leukemia that arose from further alterations in the blast population. To determine if the resistance is from the original LSCs or from new LSCs, analysis will need to be completed to identify and characterize the resistant populations. Evaluation of relapsed populations include utilization of immuno-staining, flow cytometry, and molecular analysis including assessment of TCR rearrangement to track clonality, and transplantations to compare to our untreated mouse model as well as investigation of cytogenic abnormalities, copy number variation, and gene expression profiles.

There is still much work that needs to be done to reach all of our stated objectives. Since PTEN loss and deregulated PI3K/AKT/mTOR and Myc expression are common alterations found in human T-ALL, it is important to closely mimic human PTEN-deficient T-ALL to develop alternative therapies as in this study with our *Pten* null T-ALL mouse model and cell lines. MOLT 16 is an established human cell line from a

patient with T-ALL and is characterized by a translocation of chromosome 8 and chromosome 14 [t(8;14)(q24;qll)] with the breakpoint mapped to the gene encoding the T-cell receptor α-chain (TCRA) and the 3' side of *MYC* exons (44). This translocation is analogous to the t(14;15) of our *Pten* null T-ALL model. Furthermore, this cell line is NOTCH1 WT and PTEN-deficient like our *Pten* null T-ALL. Interestingly, MOLT 16 was most sensitive of the human cell lines to our targeted therapy. To date, our data strongly indicates exploitation of these lesions through dual treatment and co-targeting of the PI3K/AKT/mTOR and Myc overexpression pathways, key pathways necessary for disease maintenance and progression, may potentially offer an improved anti-leukemic therapy to rapidly and efficiently eradicate blasts, LSCs, and ultimately human T-ALL.

REFERENCES

1. Onciu, M., *Acute Lymphoblastic Leukemia*. Hematology/Oncology Clinics of North America. Vol. 23, Issue 4, 655-674 (2009).

2. Pui, CH., et al. *Acute Lymphoblastic Leukemia*. The New England Journal of Medicine 350:15, 1535-1548 (2004).

3. Pui, CH., Jeha, S. *New therapeutic strategies for the treatment of acute lymphoblastic leukaemia*. Nature Review. Vol. 6, 149-165 (2007).

4. Aifantis, I., et al. *Molecular pathogenesis of T-cell leukaemia and lymphoma*. Nature Review Vol. 8, 380-390 (2008).

5. Gutierrez, A., et al. *High frequency of PTEN, PI3K, and AKT abnormalities in T-cell acute lymphoblastic leukemia*. Blood. Vol. 114. No. 3, 647-650 (2009).

6. Guo, W., et al., *Multi-genetic events collaboratively contribute to Pten-null leukaemia stem-cell formation*. Nature 453: 529-532 (2008)

7. Guo, W., et al., *Suppression of leukemia development caused by PTEN loss*. PNAS vol. 108, no.4, 1409-1414. (2011)

8. Kreso, A. and Dick, J., *Evolution of the Cancer Stem Cell Model*. Cell Stem Cell, 275 – 291 (2014).

9. Dick, J. *Stem cell concepts renew cancer research*. Blood. Vol. 112. No. 13, 4793-4804 (2008).

10. Huntley, B. and Gilliland, G., *Leukemia stem cells and the evolution of cancer-stem-cell research*. Nature Reviews Cancer. Vol. 5, 311-320 (2005).

11. Park, C., et. al., *Cancer Stem Cell-Directed Therapies: Recent Data From the Laboratory and Clinic.* Molecular Therapy. Vol. 17. No.2, 219-230 (2009).

12. Clevers, H., *The cancer stem cell: premises, promises, and challenges*. Nature Medicine. Vol. 17. No. 3, 313 – 320 (2011).

13. Wang, J.C.Y., *Evaluation Therapeutic Efficacy against Cancer Stem Cells: New Challenges Posed by a New Paradigm*. Cell Stem Cell, 497-501 (2007).

14. Visvader, J., *Cells of origin in cancer*. Nature Reviews. Vol. 469, 314-322 (2011).

15. Bonnet, D. and Dick, J., *Human acute myeloid leukemia is organized as a hierarchy that originates from a primitive hematopoietic cell*. Nature Medicine. Vol. 3, 730 -737 (1997).

16. Yilmaz, Ö., et. al., *Pten dependence distinguishes haematopoietic stem cells from leukemia-initiating cells.* Nature. Vol. 441, 475-482 (2006).

17. Palomero, T., et al. *Mutational loss of PTEN induces resistance to NOTCH1 inhibition in T-cell leukemia*. Nature Medicine.Vol.13. No. 10, 1203-1210 (2007).

18. Gedman. A.L., et al. *The impact of NOTCH1, FBW7, and PTEN mutations on prognosis and downstream signaling in pediatric T-cell acute lymphoblastic leukemia: a report from the Children's Oncology Group.* Nature Leukemia 23, 1417-1425. (2009).

19. Newton, R.H., et al. *Regulation of T cell homeostasis and responses by Pten*. Frontiers in Immunology. Vol.3. Article 151, (2012).

20. Kaveri, D., et al. *β-Catenin activation synergizes with Pten loss and Myc overexpression in Notch-independent T-ALL*. Blood. Vol. 122. No. 5, 694-704 (2013).

21. Ballou, Lisa., et al., *Rapamycin and mTOR Kinase Inhibitors*. J. Chem Biol. 1:27-36 (2008).

22. Kentsis, A., et . al., *Distinct and Dynamic Requirements for mTOR Signaling in Hematopoiesis and Leukemogenesis*. Cell Stem Cell. 281-282 (2012).

23. Kalaitzidis, D., et. al., *mTOR Complex 1 Plays Critical Roles in Hematopoiesis and Pten-Loss-Evoked Leukemogenesis*. Cell Press. 429-439 (2012).

24. Magee, J., et al., *Temporal Changes in PTEN and mTOR Regulation of Hematopoietic Stem Cell Self-Renewal and Leukemia Suppression*. Cell Press. 415- 428 (2012).

25. Favera, R.D., et al. *Cloning and characterization of different human sequences related to the onc gene (v-myc) of avian myelocytomatosis virus (MC29)*. PNAS, 79, 6497 – 6501 (1982).

26. Vennstrom, B., et al. *Isolation and Characterization of c-myc, a Cellular Homolog of the Oncogene (v-myc) of Avian Myelocytomatosis Virus Strain 29*. Journal of Virology, 42(3), 773-779 (1982).

27. Kato, G.J. and Dang, C.V. *Function of the c-Myc oncoprotein*. The FASEB Journal, 6, 3065 – 3072 (1992).

28. Dang, C.V. *c-Myc Target Genes Involved in Cell Growth, Apoptosis, and Metabolism*. Molecular and Cellular Biology, 19(1), 1-11. (1999).

29. Harrington, E.A., et al., *VX-680, a potent and selective small-molecule inhibitor of the Aurora kinases, suppresses tumor growth in vivo*. Nature Medicine 10, 262 - 267 (2004).

30. Yang., et al., *Therapeutic potential of a synthetic lethal interaction between the MYC proto-oncogene and inhibition of aurora-B kinase*. PNAS. Vol. 107. No.31, 13836-13841 (2010).

31. Hollander, J., et. al., *Aurora kinases A and B are up-regulated by Myc and are essential for maintenance of the malignant state*. Blood. Vol. 116. No. 9, 1498-1505 (2010).

32. Carmena, M., Earnshaw, W., *The cellular geography of aurora kinases*. Nature Reviews Molecular Cell Biology. Vol. 4, 842-854 (2003).

33. Filippakopoulos, P., et. al., *Selective inhibition of BET bromodomains*. Nature. Vol. 468, 1067-1073 (2010).

34. Zuber., et al., *RNAi screen identifies Brd4 as a therapeutic target in acute myeloid leukaemia*. Nature. Vol. 478, 524-528 (2011).

35. Delmore, J.E., et al. *BET Bromodomain Inhibition as a Therapeutic Strategy to Target c-Myc*. Cell. 146, 904-917 (2011).

36. Mertz., et al., *Targeting MYC dependence in cancer by inhibiting BET bromodomains*. PNAS. Vol. 108. No. 40, 16669-16674 (2011).

37. Ott, C., et al. *BET bromodomain inhibition targets both c-Myc and IL7R in high-risk acute lymphoblastic leukemia.* Blood. Vol. 120, No. 14, 2843-2852 (2012).

38. Dawson, M., et. al., *Inhibition of BET recruitment to chromatin as an effective treatment for MLL-fusion leukaemia*. Nature. Vol. 478, 529-533 (2011).

39. Loven, J., et. al., *Selective Inhibition of Tumor Oncogenes by Disruption of Super-Enhancers.* Cell. 153, 320-334 (2013).

40. Zhang, W., et. al., *Bromodomain-containing Protein 4 (BRD4) Regulates RNA Polymerase II Serine 2 Phosphorylation in Human CD4+ T Cells*. Journal of Biological Chemistry. Vol. 287. No. 51, 43137 – 43155 (2012).

41. Goga, A., et al. *Inhibition of CDK1 as a potential therapy for tumors over-expressing MYC*. Nature Medicine. Vol. 13. No. 7, 820-827 (2007).

42. Liu, J., et al. *Beclin1 Controls the Levels of p53 by Regulating the Deubiquitination Activity of USP10 and USP13*. Cell. 147 223-234 (2011).

43. Dail, M., et al. *Mutant Ikzf1, KrasG12D, and Notch1 cooperate in T lineage leukemogenesis and modulate responses to targeted agents*. PNAS. 107;11, 5106-11 (2010).

44. McKeithan, T., et. al.*, Molecular cloning of the breakpoint junction of a human chromosomal 8;14 translocation involving the T-cell receptor α-chain gene sequences on the 3' side of MYC.* PNAS 6636-6640 (1986).

45. O'Donnell, K., et al. *Activation of Transferrin Receptor 1 by c-Myc Enhances Cellular Proliferation and Tumorigenesis*. Molecular and Cellular Biology 2373-2386 (2006).